Article type : Original Article

3D magnetic resonance spectroscopic imaging reveals links between brain metabolites and multidimensional pain features in fibromyalgia

Jeungchan Lee,[1] Ovidiu C. Andronesi,[1] Angel Torrado-Carvajal,[1,2] Eva-Maria Ratai,[1] Marco L. Loggia,[1] Akila Weerasekera,[1] Michael P. Berry,[1] Dan-Mikael Ellingsen,[1,3] Laura Isaro,[4] Asimina Lazaridou,[4] Myrella Paschali,[4] Arvina Grahl,[1] Ajay D. Wasan,[5] Robert R. Edwards,[4] Vitaly Napadow[1,4]

Departments/institution:

[1] Department of Radiology, Athinoula A. Martinos Center for Biomedical Imaging, Massachusetts General Hospital, Harvard Medical School, Charlestown, MA 02129, USA

[2] Medical Image Analysis and Biometry Laboratory, Universidad Rey Juan Carlos, Madrid, Spain

[3] Department of Psychology, University of Oslo, Oslo, Norway

[4] Department of Anesthesiology, Perioperative and Pain Medicine, Brigham and Women's Hospital, Harvard Medical School, Boston, MA 02115, USA

[5] Department of Anesthesiology and Perioperative Medicine, Center for Innovation in Pain Care, University of Pittsburgh, Pittsburgh, PA 15261, USA

Corresponding author: Jeungchan Lee, PhD, Martinos Center for Biomedical Imaging, 149 Thirteenth Street, Suite 2301, Charlestown, MA 02129. Telephone number: +1-617-724-3402, E-mail address: jlee196@mgh.harvard.edu

Category: Original article

Running head: Brain metabolites and pain features in fibromyalgia

Funding: This work was supported by the NIH (National Institute of Arthritis and Musculoskeletal and Skin Diseases grant R01-AR064367 (VN and RRE), National Center for Complementary and Integrative Health grants R01-AT007550, R61/R33-AT009306, and P01-AT009965 (VN), and National Center for Research Resources grants P41-RR14075, S10-RR021110, and S10-RR023043). Development of MRSI pulse sequence and processing was funded by NIH/NCI grants K22CA178269 and R01CA211080 (OCA).

Conflicts of interest: We have no conflicts of interest to disclose.

Significance: This large N study linked brain metabolites and pain features in fibromyalgia patients, with a better spatial resolution and brain coverage, to understand a molecular mechanism underlying pain catastrophizing and other aspects of pain transmission. Metabolite levels in self-referential cognitive processing area as well as pain-processing regions were associated with pain outcomes. These results could help the understanding of its pathophysiology and treatment strategies for clinicians.

Abstract

Background: Fibromyalgia is a centralized multidimensional chronic pain syndrome, but its pathophysiology is not fully understood.

Methods: We applied 3D magnetic resonance spectroscopic imaging (MRSI), covering multiple cortical and subcortical brain regions, to investigate the association between neuro-metabolite (*e.g.*, combined glutamate and glutamine, Glx; myo-inositol, mIno; and combined (total) N-acetylaspartate and N-acetylaspartylglutamate; tNAA) levels and multidimensional clinical/behavioral variables (*e.g.*, pain catastrophizing, clinical pain severity, and evoked pain sensitivity) in women with fibromyalgia (N=87).

Results: Pain catastrophizing scores were positively correlated with Glx and tNAA levels in insular cortex, and negatively correlated with mIno levels in posterior cingulate cortex (PCC). Clinical pain severity was positively correlated with Glx levels in insula and PCC, and with tNAA levels in anterior midcingulate cortex (aMCC), but negatively correlated with mIno levels in aMCC and thalamus. Evoked pain sensitivity was negatively correlated with levels of tNAA in insular cortex, MCC, PCC, and thalamus.

Conclusions: These findings support single voxel placement targeting nociceptive processing areas in prior ^{1}H-MRS studies, but also highlight other areas not as commonly targeted, such as PCC, as important for chronic pain pathophysiology. Identifying target brain regions linked to multidimensional symptoms of fibromyalgia (*e.g.*, negative cognitive/affective response to pain, clinical pain, evoked pain sensitivity) may aid the development of neuromodulatory and individualized therapies. Furthermore, efficient multi-region sampling with 3D MRSI could reduce the burden of lengthy scan time for clinical research applications of molecular brain-based mechanisms supporting multidimensional aspects of fibromyalgia.

1. Introduction

Fibromyalgia (FM) is a chronic pain syndrome that is thought to result mainly from central, rather than peripheral (Fasolino et al., 2020), nervous system dysfunction. FM is diagnosed based on self-reported symptoms (without physical examination) including the number of painful body areas and both pain and non-pain symptom severity (e.g., fatigue, sleep, muscle pain) (Wolfe et al., 2010); it is commonly characterized by multidimensional symptoms, including widespread pain (Ellingsen et al., 2020; Kim et al., 2015b; Staud et al., 2007), fatigue and mood disturbance along with pain catastrophizing (Loggia et al., 2014), and augmented sensitivity (*e.g.*, enhanced temporal summation of pain) to experimental noxious stimuli (Kim et al., 2015b). Brain imaging has an important role as an objective, non-invasive tool to investigate the multidimensional brain mechanisms of FM. For instance, multiple proton magnetic resonance spectroscopy (^{1}H-MRS) studies have demonstrated altered neuro-metabolite (*e.g.*, combined glutamate and glutamine, Glx; myo-inositol, mIno; combined N-acetylaspartate and N-acetylaspartylglutamate; tNAA) concentrations in discrete nociceptive processing brain regions in FM compared to demographically-matched non-pain control samples (Aoki et al., 2013; Fayed et al., 2010; Feraco et al., 2011; Harris et al., 2009; Peek et al., 2020; Valdes et al., 2010). However, the precise linkage between metabolite concentration levels and multidimensional clinical/behavioral variables for fibromyalgia remains unknown.

The most common ^{1}H-MRS methodology is single-voxel spectroscopy (SVS), which estimates metabolic profiles from a preselected single brain region (Wilson et al., 2019), such as insular cortex (Harris et al., 2009), posterior cingulate cortex (PCC) (Fayed et al., 2012), thalamus (Feraco et al., 2011; Valdes et al., 2010). However, SVS is subject to potential bias in single region-preselection and is time-consuming if data collection is needed from multiple brain regions (Gussew et al., 2011; Lv et al., 2018). In contrast, 3D MR spectroscopic imaging (MRSI) investigates metabolic profiles from multiple brain regions simultaneously (Maudsley et al., 2020). However, non-uniform data quality across all sampled regions and across all metabolites may be a weakness of MRSI, and difficulty in visual inspection of data quality highlights the need for an automated quality-control pipeline (Wilson et al., 2019). Thus, while MRSI has shown promise for many clinical applications (Al-Iedani et al., 2020; Andronesi et al., 2020), only a few pain studies (*e.g.*, FM (Petrou et al., 2008) and idiopathic trigeminal neuralgia (Wang

et al., 2014)) have applied single-slice 2D MRSI methods. Moreover, none of previous studies have used 3D MRSI or implemented data quality assessment procedures in chronic pain.

We applied multi-slice voxel-wise 3D MRSI to link brain metabolite (*e.g.*, Glx, mIno, and tNAA) concentrations across numerous brain regions to multidimensional symptoms reported by FM patients (*e.g.*, pain catastrophizing, clinical pain intensity, and evoked pain sensitivity). We also applied an automated data-quality assessment procedure which adopted an inpainting technique (Torrado-Carvajal et al., 2020) to restore low-quality data voxels and achieve better coverage across the brain. We hypothesized that concentration levels of metabolites in cognitive/affective- and pain-processing brain regions would be correlated with multidimensional clinical/behavioral variables in FM.

2. Methods

This study was approved by the Partners Human Research Committee, and the experiment was performed at the A. A. Martinos Center for Biomedical Imaging in Boston, Massachusetts, in accordance with the principles of the Declaration of Helsinki. All enrolled participants were fully informed of the detailed procedure of this study and provided written informed consent. Participants were de-identified by numeric codes.

2.1. Participants

Eighty-seven (N = 87) female FM patients (age = 40.7 ± 12.2 years, mean ± SD), who met the American College of Rheumatology (ACR) criteria for a diagnosis of FM (Wolfe et al., 2010), were enrolled in this study. All patients were screened by phone prior to a behavioral visit which determined study eligibility, meeting the following inclusion criteria: (1) female (due to predominance of female sex for diagnosed fibromyalgia (Castel et al., 2013; Lourenco et al., 2015)), (2) age between 18 and 65 years, (3) meeting the ACR diagnostic criteria for FM for more than 1 year, (4) stable dose for all medications, (5) reporting moderate to severe FM pain intensity on average (at least 4 of 10 on a 0-10 Numeric Rating Scale), (6) pain on at least 50% of days, and (7) fluency in English with ability to provide written informed consent. We excluded patients from the study if they met the following exclusion criteria (assessed by self-report): (1) comorbid acute/chronic pain conditions with pain severity greater than FM pain, (2) usage of stimulant medications for fatigue, sleep apnea, or shift work, (3) current or recent usage of recreational drugs, (4) suffering from any psychiatric disorders that included a history of psychotic symptoms (*e.g.*, schizophrenia), (5) psychiatric hospitalization within 6 months prior to enrollment, (6) active suicidal ideation, (7) participation in other therapeutic trials at the same time (FM participants were enrolled as part of a longitudinal neuroimaging study), (8) lower limb vascular surgery or current lower limb vascular dysfunction, (9) pregnant or nursing, (10) history of significant head injury (*e.g.*, loss of consciousness), (11) anxiety disorders interfering with MRI experimental procedures (*e.g.*, panic), or (12) other contraindications for MRI. In order to better contextualize the findings in the FM group, sex/age-matched healthy controls (HC) were recruited (N = 40 women, age = 39.8 ± 13.5 years, P = 0.72, unpaired *t*-test contrasting FM and HC) and compared with FM patients in this study.

All participants (*i.e.*, FM and HC) completed a separate behavioral visit prior to the MRI/MRSI session, during which they were given an overview of study procedures and completed questionnaires: the Pain Catastrophizing Scale (PCS) was administered as a measure of negative cognitive/affective responses to pain (Sullivan et al., 1995), and the Brief Pain Inventory (BPI, FM only) provided a measure of clinical pain intensity (Cleeland and Ryan 1994). We also assessed evoked pain sensitivity via cuff pain algometry (as in prior studies (Hubbard et al., 2020; Kim et al., 2015b; Loggia et al., 2014)) by assessing the Cuff P40 pressure (mmHg at which pain intensity ~ 40/100, 0 = no pain, 100 = worst pain imaginable) with an E20 Rapid Cuff Inflation System (D. E. Hokanson, Inc.) at the MRI session. Similar to our prior studies (Hubbard et al., 2020; Kim et al., 2015b; Loggia et al., 2014) which linked functional brain responses to evoked cuff pain, the pressure (mmHg) was individually tailored at the left lower leg (with the cuff centered around the point of largest calf circumference) to a target pain intensity rating (40 out of 100). Patients reported FM duration (years) and pain intensity at study visit (0 to 100), and completed the following validated questionnaires: revised Fibromyalgia Impact Questionnaire (FIQR) (Bennett et al., 2009), painDETECT (Freynhagen et al., 2006; Freynhagen et al., 2016), and the Patient-Reported Outcomes Measurement Information System (PROMIS-29) questionnaire (Katz et al., 2017).

2.2. Magnetic resonance spectroscopic imaging (MRSI) data acquisition

MRSI data, as well as structural brain MRI, were collected using a 3.0 Tesla MRI scanner (Skyra, Siemens Medical, Germany) equipped with a 32-channel head coil. MRSI was performed with a custom-developed (Andronesi et al., 2012; Bogner et al., 2014) pulse sequence using localized adiabatic spin-echo refocusing (LASER) excitation and spiral spatial-spectral (k,t) encoding (TR/TE = 1500/30 ms, FOV = 240 mm × 240 mm × 151 mm, acquired matrix = 19 × 19 × 12, acquired voxel size = 12.5 mm × 12.5 mm × 12.5 mm, zero-filled reconstructed matrix = 32 × 32 × 16, reconstructed voxel size = 7.5 mm × 7.5 mm × 7.5 mm, spectral window = 1250 Hz, number of time points = 320, zero-filled to 512, number of averages = 2, acquisition time = 3 min 42 s) to assess metabolic concentration within cortical and subcortical regions of the brain. The acquisition time was kept under 4 minutes due to the potential for patient discomfort, as the total scan session time needed to be kept to a feasible time limit (~ 1.5 hours) for FM patients. Longer scan times can also lead to head motion during the scan, which compromises data quality.

Water suppression was included in the pulse sequence as WET (water suppression enhanced though T1 effects). B_0 shimming using a B_0 field-mapping technique, as implemented by the vendor, was used and provided a global linewidth for the water less than 15 Hz over the entire VOI. The carrier of the RF pulses was set at 3 ppm, which is in the center of the chemical shift interval of interest (2 – 4 ppm). The MRSI volume of interest (VOI, 90 mm × 100 mm × 50 mm) was placed over the structural MRI image reference to cover the bilateral insular and cingulate cortices, thalami, and basal ganglia, while excluding subcutaneous fat to avoid lipid contamination of MRSI data (Wilson et al., 2019). T1-weighted structure images were also collected using a 3D MP-RAGE pulse sequence (TR/TE = 2530/1.64 ms, FOV = 256 mm × 256 mm, spatial resolution = 1 mm × 1 mm × 1 mm, flip angle = 7°), which facilitated placement of the MRSI VOI, gray matter segmentation, and co-registration of individual MRSI data to the MNI common space.

2.3. Data processing and analysis

MR spectra for each voxel were model fit using LCModel (version 6.3-1L, http://s-provencher.com) (Provencher 1993) with the default macromolecules to estimate metabolite concentrations for total Cr (tCr, combined creatine and phosphocreatine), Glx (combined glutamate and glutamine), mIno (myo-inositol), and total NAA (tNAA, combined N-acetylaspartate and N-acetylaspartylglutamate). The simulated basis sets used to fit acquired spectra included ascorbic acid, aspartate, creatine, N-acetylaspartate, N-acetylaspartylglutamate, gamma-aminobutyric acid, glucose, glutamate, glutamine, glutathione, glycerophosphocholine, glycine, 2-hydroglutarate, mIno, scyllo-inositol, taurine, phosphocholine, phosphocreatine, phosphoethanolamine, tNAA, mIno+glycine, tCr, and Glx. Metabolic concentration and quality maps were created after LCModel fitting using a custom processing pipeline based on Matlab, MINC and FSL software as we described previously (Bogner et al., 2014).

In order to perform group analyses, we first defined ‘adequate’- and ‘low’-quality data voxels for each metabolite and voxel spectrum based on the following LCModel outputs: signal-to-noise ratio (SNR, calculated by dividing the signal intensity of NAA by that of the noise level) (Provencher 1993), full width at half maximum (FWHM), and Cramer-Rao lower bounds (CRLB). In this study these data quality thresholds for SNR, FWHM, and CRLB were 5 (Andronesi et al., 2018; Andronesi et al., 2012), 0.1 ppm (*i.e.*, 12.3 Hz) (Andronesi et al., 2018),

and 20% (Lv et al., 2018), respectively. Thus, the voxels with SNR ≥ 5, FWHM < 0.1 ppm, *and* CRLB < 20% were classified as 'adequate'-quality data voxels, while voxels with SNR < 5, FWHM ≥ 0.1 ppm, *or* CRLB ≥ 20% were categorized as 'low'-quality data voxels.

As our MRSI technique produced some 'low'-quality data voxels (for Glx, mIno, and tNAA maps), such voxels were restored (on the 3D metabolic maps, not the raw spectra) over the VOI using an inpainting algorithm (Torrado-Carvajal et al., 2020). This was completed to include as many voxels as possible in the analyses, allowing for a whole-VOI MRSI analysis instead of excluding voxels from the analysis. Briefly, as the 'low'-quality data voxel regions in metabolite concentration maps usually contain structure and texture information, the inpainting algorithm provides a better estimation of missing/corrupted values than other traditional interpolation algorithms by using discrete cosine transform-based penalized least square regression (DCT-PLS) (Criminisi et al., 2004; Garcia 2010), which considers both global and local properties of an image. For example, the inpainting algorithm applied to a sample human MRSI (*i.e.*, NAA) dataset showed the lowest error scores (with an average normalized root mean square error < 5%, even when inpainting up to 50% missing voxels) compared with more conventional nearest neighbor, polynomial, and cubic interpolations (Torrado-Carvajal et al., 2020).

For each subject, the inpainted metabolite concentration maps for Glx, mIno, and tNAA were then normalized by tCr (Archibald et al., 2020; Ratai et al., 2018; Wilson et al., 2019), which was defined as the average tCr value over all 'adequate' VOI gray matter voxels (using the Freesurfer segmentation (Fischl et al., 2002)). The normalized, inpainted maps were registered to the subject's T1-weighted structural volume (FLIRT, FSL) and then co-registered to standard space (Montreal Neurological Institute, MNI; FNIRT, FSL) for group analysis, where the MNI152 template was resampled into 7.5 mm isotropic voxels to match the native MRSI spatial resolution. Data analysis was performed only for voxels with contribution (*i.e.*, aligned MRSI VOI brain coverage) from all of participants.

As we calculated the average tCr value over all VOI gray matter voxels with 'adequate' data quality for normalization, average metabolite values for Glx, mIno, and tNAA were calculated in the same way for each subject. Outlier metabolites were defined in each subject by an average metabolite-to-tCr value greater or less than 3 standard deviations from the group mean, and those outlier metabolites were excluded from group analyses.

Binarized 'low'-quality voxel maps, which indicate the location of voxels to be interpolated (0 = 'adequate', 1 = 'low'-quality voxel), were created in native (raw) data space based on SNR, FWHM, and CRLB thresholds for Glx, mIno, and tNAA, as noted above. These maps were also co-registered to standard space in order to estimate the location of interpolated voxels and the percentage of inpainted voxels across all subjects.

For group analyses in FM, whole-VOI voxel-wise multiple linear regression analysis was performed for clinical/behavioral variables (*i.e.*, PCS, BPI severity, and Cuff P40 pressure), controlling for patients' age (known to be associated with metabolite levels) (Clauw 2014; Erickson et al., 2015; Fayed et al., 2014), usage of medications known to affect Glx levels (*i.e.*, gabapentin and pregabalin) (Clauw 2014; De Jaeger et al., 2018; Harris et al., 2013), and average tCr levels (Pearson's r with PCS = 0.26, P = 0.015; r with BPI severity = 0.33, P = 0.002; and r with Cuff P40 pressure = -0.01, P = 0.912). These group-level analyses used a mixed-effects model with Ordinary Least Squares (OLS, FEAT, FSL) and were cluster-corrected for multiple comparisons ($Z > 2.3$, $P < 0.05$). Additionally, due to the exploratory nature of this study, we also include the uncorrected results that passed our uncorrected criteria. Each voxel from this regression analysis was considered significant if all of the following 3 criteria were met: (1) the corresponding uncorrected absolute Z statistic value was equal to or greater than 2.3, (2) the percentage of subjects with inpainted data at that specific voxel (in MNI space) was less than 60%, *and* (3) the significant correlation between metabolite and clinical/behavioral variables (*i.e.*, PCS, BPI severity, or Cuff P40 pressure) was still significant ($P \leq 0.05$) when outliers and inpainted data subjects were excluded (*i.e.*, only using the subset of subjects with 'adequate'-quality data).

Group differences between FM and HC in clinical/behavioral variables (*i.e.*, PCS and Cuff P40 pressure) and metabolite levels (*i.e.*, Glx/tCr, mIno/tCr, and tNAA/tCr) were also assessed. For clinical and behavioral variables, a Kolmogorov-Smirnov test was first applied to test the normality of the data, and a Student's two-sample unpaired *t*-test was performed ($P \leq 0.05$ was considered as significant) for normally distributed variables. For MRSI data, whole-VOI voxel-wise analysis (unpaired two-group difference) was performed using a mixed-effects model with OLS (FEAT, FSL) (significance determined by criteria 1 and 2, above).

3. Results

All clinical and behavioral variables collected in this study were normally distributed (P's > 0.09). Compared with HC, FM patients reported significantly higher pain catastrophizing scores (PCS: FM = 24.1 ± 11.6, HC = 8.1 ± 8.0, P < 0.003) and lower cuff P40 pressure (FM = 147.0 ± 52.8 mmHg, HC = 184.6 ± 72.1 mmHg, P < 0.003). FM patients reported moderate pain severity (BPI severity: FM = 5.1 ± 1.7) (**Table 1**). In FM, PCS was positively correlated with BPI severity (r = 0.60, P < 0.0001, N = 86). Cuff P40 pressure, however, was not correlated with PCS (r = -0.004, P = 0.976, N = 75) or with BPI severity (r = -0.11, P = 0.329, N = 75). There was also no significant correlation between PCS and Cuff P40 pressure in HC (r = 0.10, P = 0.597, N = 32).

[Table 1 here]

VOI placement for MRSI data collection successfully covered targeted brain regions such as bilateral insular and cingulate cortices, thalami, and basal ganglia (**Fig. 1a**) with good spectral fits (**Fig. 1b**). Of 87 FM patients, metabolite outlier rejection eliminated one patient from Glx/tCr analysis and two patients from mIno/tCr analysis; thus, 86 FM patients were analyzed for Glx/tCr, 85 FM patients for mIno/tCr, and 87 for tNAA/tCr. Nineteen (N = 19) FM patients reported that they had taken medications such as gabapentin or pregabalin; use of these medications was statistically controlled for in analyses. Six HC, of the 40, were excluded due to lingering pain during the MRSI data collection from pre-existing maladies (*e.g.*, plantar fasciitis and shoulder injury), and one additional HC was removed from the analysis after reporting recent use of gabapentin. After outlier rejection for metabolite levels, two HC were excluded from metabolite analysis. (**Fig. 2**).

[Figure 1 here]

[Figure 2 here]

The majority of 'low'-quality data voxels (SNR < 5, FWHM ≥ 0.1 ppm, *or* CRLB ≥ 20%) were located in the ventromedial part of the VOI (including the subgenual anterior cingulate

cortex, the genu and rostrum of corpus callosum, which are affected by B_0 inhomogeneity) and in the ventricles of the brain (**Fig. 3**).

[Figure 3 here]

In group comparisons between FM and HC, we found greater mIno/tCr levels in the right posterior supramarginal gyrus (Z score = 2.36, MNI coordinates: X = 33 mm, Y = -39.75 mm, Z = 37.5 mm, %inpaint = 15% in FM and 29% in HC, P('adequate'-quality data voxels only) = 0.046) and smaller tNAA/tCr levels in the right posterior cingulate cortex (Z score = -2.57, MNI coordinates: X = 3 mm, Y = -32.25 mm, Z = 22.5 mm, %inpaint = 5% in FM and 0% in HC, P('adequate'-quality data voxels only) = 0.005), but there were no significant differences in Glx/tCr concentration levels in any regions (**Fig. S1**).

In voxel-wise multiple linear regression analysis in the FM group, we found significant positive correlations between PCS score and Glx/tCr concentration in the anterior and middle insular cortices (**Table 2, Fig. 4a**). Glx/tCr levels in the middle/posterior insular and posterior cingulate cortices were positively correlated with BPI severity (**Fig. 4b**). The level of mIno/tCr in the posterior cingulate cortex was negatively correlated with PCS score (**Fig. 5a**), where their levels in the anterior cingulate cortex (ACC) and thalamus were negatively correlated with BPI severity scores (**Fig. 5b**). Interestingly, Cuff P40 pressures were not correlated with either Glx/tCr or mIno/tCr levels at any voxels in the VOI. PCS was positively correlated with tNAA/tCr levels in the anterior and middle insular cortices (**Fig. 6a**), while BPI severity was negatively correlated with tNAA/tCr levels in the ACC (**Fig. 6b**). Finally, Cuff P40 pressure was positively correlated with tNAA/tCr levels in the posterior insular cortex, middle and posterior cingulate cortices, and thalamus (**Fig. 6c**).

[Table 2 here]

[Figure 4 here]

[Figure 5 here]

[Figure 6 here]

4. Discussion

Fibromyalgia (FM) is a centralized pain condition characterized by impaired pain processing in the brain (*e.g.*, pain amplification or facilitated nociception) (Clauw 2014; Peek et al., 2020; Petrou et al., 2008). An underlying mechanism for facilitated pain transmission in the brain may be altered levels of neurotransmitters and other molecular mediators of neural activity (Clauw 2014; Wang et al., 2014). In this study, we evaluated brain metabolites in a large sample of FM patients using a voxel-wise 3D MRSI technique. FM patients exhibited greater mIno/tCr levels in the right posterior supramarginal gyrus and lower tNAA/tCr levels in the right posterior cingulate cortex. We then identified significant associations between clinical/behavioral variables and metabolite levels (*i.e.*, Glx/tCr, mIno/tCr, and tNAA/tCr) in both sensory/nociception-processing (*i.e.*, insular and anterior cingulate cortices, thalamus) (Coghill 2020) and self-referential cognitive processing areas (*e.g.*, PCC) (Lee et al., 2018). These results highlight the utility of MRSI in the assessment of molecular mechanisms underlying pain catastrophizing and other aspects of pain transmission in FM. Also, our findings not only support prior and ongoing chronic pain single-voxel ^{1}H-MRS studies that assess metabolites from consistently-identified sensory/nociception-processing brain areas (Coghill 2020) but highlight other areas, such as PCC, as important for chronic pain pathophysiology.

Our study found positive associations between Glx levels in the anterior and middle insular cortices and PCS scores. Glx levels in middle/posterior insular and posterior cingulate cortices were positively associated with BPI severity scores. Anterior insular cortex is an important node for affective/salience processing of the pain experience, while posterior insular cortex is known to play a crucial role in nociceptive processing (Frot et al., 2014; Lee et al., 2019; Lu et al., 2016; Morel et al., 2013; Napadow et al., 2010). Thus, the associations between (1) cognitive-affective dimensions of chronic pain (*i.e.*, PCS) and Glx levels in the anterior/middle insular cortex and (2) sensory/physical aspects of pain (*i.e.*, BPI) and Glx levels in the middle/posterior insular cortex, are in line with the distinct role of anterior (Bednarska et al., 2019) versus posterior (Harfeldt et al., 2018; Harris et al., 2013; Harris et al., 2009) insular processing for pain. Furthermore, our recent fMRI study in patients with chronic low back pain (cLBP) found that catastrophizing mediated the association between clinical pain and default mode network (DMN) connectivity to the anterior/middle insular cortex (Kim et al., 2019). A recent study also found that fMRI response to heat pain was positively correlated with Glx

concentration in anterior/middle insular cortex (Cleve et al., 2017), similarly to fMRI response to visual stimulation and Glx concentration in the occipital lobe (Boillat et al., 2020; Ip et al., 2017). These studies suggest that greater Glx levels either allow for or result from greater neuronal and hemodynamic response to evoked stimuli. Our previous study found that engaging in pain catastrophizing by FM patients activates DMN regions, specifically PCC (Lee et al., 2018). Thus, the association in this study between Glx levels in anterior/middle insular cortex and PCS suggests that our previous findings of greater functional coupling between DMN and anterior/middle insular cortex in chronic pain patients, particularly in high PCS chronic pain patients (Kim et al., 2019), and its linkage to the clinical pain state (Kim et al., 2019; Loggia et al., 2013; Napadow et al., 2010), may be supported by PCS-linked elevated Glx levels in regions such as anterior/middle insular cortex.

Levels of mIno in ^{1}H-MRS studies have been suggested to represent markers for glial activity and neuroinflammation (Simis et al., 2015), though others have debated this linkage (Chang et al., 2013; Rae 2014) and our group did not find elevated insula mIno levels in a different cohort of FM patients (Jung et al., 2020). However, we found greater mIno levels for FM in right posterior supramarginal gyrus. Our group previously reported widespread neuroinflammation in FM and elevated [^{11}C]PBR28 binding in this same brain region (Albrecht et al., 2019a), which was positively correlated with mIno levels (Ratai et al., 2018), thereby linking mIno and neuroinflammation in FM. We also found negative associations between mIno levels in PCC and PCS scores, and mIno levels in both anterior midcingulate cortex (aMCC) and thalamus and BPI severity. These findings are in line with a previous study in cLBP patients that reported a negative correlation between depression/anxiety levels and mIno levels in aMCC (Kameda et al., 2018), and with studies reporting decreased mIno levels in aMCC (Chiappelli et al., 2015) and pregenual ACC (Coupland et al., 2005) in major depression disorder (MDD) patients, where depression and anxiety are closely related to clinical pain (Meints et al., 2019; Mok and Lee 2008). There are, however, contradictory prior ^{1}H-MRS studies in FM (Feraco et al., 2011; Valdes et al., 2010) and pelvic pain (Simis et al., 2015), which found positive correlations between thalamic mIno concentration and pain severity. Also, previous position emission tomography (PET) studies in cLBP (Albrecht et al., 2019b) and MDD (Setiawan et al., 2015) showed positive associations between depression scores and neuroinflammation metrics in aMCC. Thus, more research is needed to assess the specific role of mIno in chronic pain.

Total NAA is thought to be a marker for neuronal density and function (Rae 2014). We found that tNAA levels in anterior/posterior midcingulate cortex (a/pMCC), posterior insular cortex, and thalamus were negatively correlated with clinical pain intensity (*i.e.*, BPI severity) and pain sensitivity (*i.e.*, positive correlation with Cuff P40 pressure). Prior study in trigeminal neuralgia patients found a negative correlation between thalamus tNAA levels (also reduced relative to HC) and facial pain intensity (Wang et al., 2014), and another study in chronic pelvic pain patients reported a negative correlation between a/pMCC tNAA levels and pressure pain sensitivity (Simis et al., 2015). Combined, these results support the hypothesis that lower tNAA levels reflect neuronal loss/dysfunction in pain/nociceptive processing areas, and reduced tNAA levels in pain patients, compared to HC, particularly in nociceptive-processing areas (*e.g.*, thalamus, aMCC), have been reported by many studies (Fayed et al., 2014; Kameda et al., 2018; Sorensen et al., 2008; Wang et al., 2014).

Conversely, we also found a positive correlation between tNAA levels in anterior/middle insular cortex and PCS scores. This finding suggests elevated neuronal density required for increased ruminative processing. Interestingly, at the same voxel location, Glx levels were also positively correlated with PCS scores. When directly correlating Glx and tNAA in the anterior/middle insular cortex, we found significant positive correlations across most voxels (R's > 0.72), suggesting that in chronic pain, any excitotoxicity has not (yet) produced neuronal loss, perhaps due to the cyclical nature of pain catastrophizing and ruminative processing rather than a constant, biologically maladaptive elevation in glutamatergic activity. On the other hand, NAA has also been considered as a mitochondrial marker, hence a decreased NAA levels might indicate a mitochondrial dysfunction (Arun et al., 2006; Madhavarao et al., 2003; Nordengen et al., 2015). Thus, the role of tNAA in chronic pain may not only relate to neuronal density but also mitochondrial function.

Some limitations of our study should be noted. Our data were collected using a 3D MRSI sequence which proved challenging to guarantee good data quality across all collected voxels. This challenge is due to an inhomogeneity of the B_0 field in a large 3D MRSI brain volume (Maudsley et al., 2020) which is more difficult to shim (Juchem et al., 2020) than in the case of single voxel ^{1}H-MRS (Oz et al., 2020). In particular, voxels in the ventromedial part of the VOI, such as subgenual ACC, were severely affected by B_0 inhomogeneity due to proximity to large air cavities (pharynx, frontal and sphenoid sinuses). To address low-quality data voxels, we

devised a post-processing method, which recovered excluded low-quality voxels by an advanced inpainting algorithm in order to allow multi-voxel group analyses using standardized fMRI analysis software. Our study adopted the concept of 'adequate'- and 'low'-quality data voxels for MRSI quality assessment. The percentage of low-quality voxels in our VOI should be compared with data collected in future studies to further assess the stability and generalizability of our approach. Due to the exploratory nature of our study, we reported results both cluster-corrected for multiple comparisons and uncorrected results. Multiple results did not survive cluster-correction, potentially due to 1) more spatially constrained locus for metabolite modulation (compared to vascular-based BOLD fMRI, the neuroimaging field from which typical cluster correction methods are derived), or 2) variability between FM subtypes. Thus, additional studies are needed to confirm our findings.

In summary, our findings not only support single voxel placement targeting nociceptive processing areas in prior ^{1}H-MRS studies, but also highlight other areas not as commonly targeted, such as PCC, as important for chronic pain pathophysiology. Identifying target brain regions linked to multidimensional symptoms of fibromyalgia (*e.g.*, negative cognitive/affective response to pain, clinical pain, evoked pain sensitivity) may aid the development of neuromodulatory and individualized therapies. Furthermore, efficient multi-region sampling with 3D MRSI could reduce the burden of lengthy scan time for clinical research applications of molecular brain-based mechanisms supporting multidimensional aspects of fibromyalgia.

Author contributions: Ajay D. Wasan, Robert R. Edwards, and Vitaly Napadow contributed to conception and design; Jeungchan Lee, Michael P. Berry, Dan-Mikael Ellingsen, Laura Isaro, Asimina Lazaridou, Myrella Paschali, and Arvina Grahl to data acquisition; Jeungchan Lee to data analysis; Jeungchan Lee, Ovidiu C. Andronesi, Angel Torrado-Carvajal, Eva-Maria Ratai, Marco L. Loggia, Akila Weerasekera, Robert R. Edwards, and Vitaly Napadow to data interpretation. Jeungchan Lee, Robert R. Edwards, and Vitaly Napadow drafted the article and all other coauthors revised it critically. All authors provided the final approval of the version to be published.

References

Al-Iedani, O., Ribbons, K., Gholizadeh, N., Lechner-Scott, J., Quadrelli, S., Lea, R., . . . Ramadan, S. (2020). Spiral MRSI and tissue segmentation of normal-appearing white matter and white matter lesions in relapsing remitting multiple sclerosis patients(). *Magn Reson Imaging*, 74, 21-30. doi:10.1016/j.mri.2020.09.001

Albrecht, D. S., Forsberg, A., Sandstrom, A., Bergan, C., Kadetoff, D., Protsenko, E., . . . Loggia, M. L. (2019a). Brain glial activation in fibromyalgia - A multi-site positron emission tomography investigation. *Brain Behav Immun*, 75, 72-83. doi:10.1016/j.bbi.2018.09.018

Albrecht, D. S., Kim, M., Akeju, O., Torrado-Carvajal, A., Edwards, R. R., Zhang, Y., . . . Loggia, M. L. (2019b). The neuroinflammatory component of negative affect in patients with chronic pain. *Mol Psychiatry*. doi:10.1038/s41380-019-0433-1

Andronesi, C. O., Nicholson, K., Jafari-Khouzani, K., Bogner, W., Wang, J., Chan, J., . . . Ratai, E.-M. (2020). Imaging neurochemistry and brain structure tracks clinical decline and mechanisms of ALS in patients. *Frontiers in Neurology*, in press.

Andronesi, O. C., Arrillaga-Romany, I. C., Ly, K. I., Bogner, W., Ratai, E. M., Reitz, K., . . . Batchelor, T. T. (2018). Pharmacodynamics of mutant-IDH1 inhibitors in glioma patients probed by in vivo 3D MRS imaging of 2-hydroxyglutarate. *Nat Commun*, 9(1), 1474. doi:10.1038/s41467-018-03905-6

Andronesi, O. C., Gagoski, B. A., & Sorensen, A. G. (2012). Neurologic 3D MR spectroscopic imaging with low-power adiabatic pulses and fast spiral acquisition. *Radiology*, 262(2), 647-661. doi:10.1148/radiol.11110277

Aoki, Y., Inokuchi, R., & Suwa, H. (2013). Reduced N-acetylaspartate in the hippocampus in patients with fibromyalgia: a meta-analysis. *Psychiatry Res*, 213(3), 242-248. doi:10.1016/j.pscychresns.2013.03.008

Archibald, J., MacMillan, E. L., Enzler, A., Jutzeler, C. R., Schweinhardt, P., & Kramer, J. L. K. (2020). Excitatory and inhibitory responses in the brain to experimental pain: A systematic review of MR spectroscopy studies. *Neuroimage*, 215, 116794. doi:10.1016/j.neuroimage.2020.116794

Arun, P., Madhavarao, C. N., Moffett, J. R., & Namboodiri, M. A. (2006). Regulation of N-acetylaspartate and N-acetylaspartylglutamate biosynthesis by protein kinase activators. *J Neurochem*, 98(6), 2034-2042. doi:10.1111/j.1471-4159.2006.04068.x

Bednarska, O., Icenhour, A., Tapper, S., Witt, S. T., Tisell, A., Lundberg, P., . . . Walter, S. (2019). Reduced excitatory neurotransmitter levels in anterior insulae are associated with abdominal pain in irritable bowel syndrome. *Pain*, 160(9), 2004-2012. doi:10.1097/j.pain.0000000000001589

Bennett, R. M., Friend, R., Jones, K. D., Ward, R., Han, B. K., & Ross, R. L. (2009). The Revised Fibromyalgia Impact Questionnaire (FIQR): validation and psychometric properties. *Arthritis Res Ther*, 11(4), R120. doi:10.1186/ar2783

Bogner, W., Hess, A. T., Gagoski, B., Tisdall, M. D., van der Kouwe, A. J., Trattnig, S., . . . Andronesi, O. C. (2014). Real-time motion- and B0-correction for LASER-localized spiral-accelerated 3D-MRSI of the brain at 3T. *Neuroimage*, 88, 22-31. doi:10.1016/j.neuroimage.2013.09.034

Boillat, Y., Xin, L., van der Zwaag, W., & Gruetter, R. (2020). Metabolite concentration changes associated with positive and negative BOLD responses in the human visual cortex: A functional MRS study at 7 Tesla. *J Cereb Blood Flow Metab*, 40(3), 488-500. doi:10.1177/0271678X19831022

Castel, A., Fontova, R., Montull, S., Perinan, R., Poveda, M. J., Miralles, I., . . . Rull, M. (2013). Efficacy of a multidisciplinary fibromyalgia treatment adapted for women with low educational levels: a randomized controlled trial. *Arthritis Care Res (Hoboken)*, 65(3), 421-431. doi:10.1002/acr.21818

Chang, L., Munsaka, S. M., Kraft-Terry, S., & Ernst, T. (2013). Magnetic resonance spectroscopy to assess neuroinflammation and neuropathic pain. *J Neuroimmune Pharmacol*, 8(3), 576-593. doi:10.1007/s11481-013-9460-x

Chiappelli, J., Rowland, L. M., Wijtenburg, S. A., Muellerklein, F., Tagamets, M., McMahon, R. P., . . . Hong, L. E. (2015). Evaluation of Myo-Inositol as a Potential Biomarker for Depression in Schizophrenia. *Neuropsychopharmacology*, 40(9), 2157-2164. doi:10.1038/npp.2015.57

Clauw, D. J. (2014). Fibromyalgia: a clinical review. *JAMA*, 311(15), 1547-1555. doi:10.1001/jama.2014.3266

Cleeland, C. S., & Ryan, K. M. (1994). Pain assessment: global use of the Brief Pain Inventory. *Ann Acad Med Singap*, 23(2), 129-138.

Cleve, M., Gussew, A., Wagner, G., Bar, K. J., & Reichenbach, J. R. (2017). Assessment of intra- and inter-regional interrelations between GABA+, Glx and BOLD during pain perception in the human brain - A combined (1)H fMRS and fMRI study. *Neuroscience*, 365, 125-136. doi:10.1016/j.neuroscience.2017.09.037

Coghill, R. C. (2020). The Distributed Nociceptive System: A Framework for Understanding Pain. *Trends Neurosci*, 43(10), 780-794. doi:10.1016/j.tins.2020.07.004

Coupland, N. J., Ogilvie, C. J., Hegadoren, K. M., Seres, P., Hanstock, C. C., & Allen, P. S. (2005). Decreased prefrontal Myo-inositol in major depressive disorder. *Biol Psychiatry*, 57(12), 1526-1534. doi:10.1016/j.biopsych.2005.02.027

Criminisi, A., Perez, P., & Toyama, K. (2004). Region filling and object removal by exemplar-based image inpainting. *IEEE Trans Image Process*, 13(9), 1200-1212. doi:10.1109/tip.2004.833105

De Jaeger, M., Goudman, L., Van Schuerbeek, P., De Mey, J., Keymeulen, B., Brouns, R., & Moens, M. (2018). Cerebral Biochemical Effect of Pregabalin in Patients with Painful Diabetic Neuropathy: A Randomized Controlled Trial. *Diabetes Ther*, 9(4), 1591-1604. doi:10.1007/s13300-018-0460-y

Ellingsen, D. M., Beissner, F., Alsady, T. M., Lazaridou, A., Paschali, M., Berry, M., . . . Napadow, V. (2020). A picture is worth a thousand words: linking fibromyalgia pain widespreadness from digital pain drawings with pain catastrophizing and brain cross-network connectivity. *Pain*. doi:10.1097/j.pain.0000000000002134

Erickson, K. I., Leckie, R. L., Weinstein, A. M., Radchenkova, P., Sutton, B. P., Prakash, R. S., . . . Kramer, A. F. (2015). Education mitigates age-related decline in N-Acetylaspartate levels. *Brain Behav*, 5(3), e00311. doi:10.1002/brb3.311

Fasolino, A., Di Stefano, G., Leone, C., Galosi, E., Gioia, C., Lucchino, B., . . . Truini, A. (2020). Small-fibre pathology has no impact on somatosensory system function in patients with fibromyalgia. *Pain*, 161(10), 2385-2393. doi:10.1097/j.pain.0000000000001920

Fayed, N., Andres, E., Rojas, G., Moreno, S., Serrano-Blanco, A., Roca, M., & Garcia-Campayo, J. (2012). Brain dysfunction in fibromyalgia and somatization disorder using proton magnetic resonance spectroscopy: a controlled study. *Acta Psychiatr Scand*, 126(2), 115-125. doi:10.1111/j.1600-0447.2011.01820.x

Fayed, N., Andres, E., Viguera, L., Modrego, P. J., & Garcia-Campayo, J. (2014). Higher glutamate+glutamine and reduction of N-acetylaspartate in posterior cingulate according to age range in patients with cognitive impairment and/or pain. *Acad Radiol*, 21(9), 1211-1217. doi:10.1016/j.acra.2014.04.009

Fayed, N., Garcia-Campayo, J., Magallon, R., Andres-Bergareche, H., Luciano, J. V., Andres, E., & Beltran, J. (2010). Localized 1H-NMR spectroscopy in patients with fibromyalgia: a controlled study of changes in cerebral glutamate/glutamine, inositol, choline, and N-acetylaspartate. *Arthritis Res Ther*, 12(4), R134. doi:10.1186/ar3072

Feraco, P., Bacci, A., Pedrabissi, F., Passamonti, L., Zampogna, G., Pedrabissi, F., . . . Leonardi, M. (2011). Metabolic abnormalities in pain-processing regions of patients with fibromyalgia: a 3T MR spectroscopy study. *AJNR Am J Neuroradiol*, 32(9), 1585-1590. doi:10.3174/ajnr.A2550

Fischl, B., Salat, D. H., Busa, E., Albert, M., Dieterich, M., Haselgrove, C., . . . Dale, A. M. (2002). Whole brain segmentation: automated labeling of neuroanatomical structures in the human brain. *Neuron*, 33(3), 341-355. doi:10.1016/s0896-6273(02)00569-x

Freynhagen, R., Baron, R., Gockel, U., & Tolle, T. R. (2006). painDETECT: a new screening questionnaire to identify neuropathic components in patients with back pain. *Curr Med Res Opin*, 22(10), 1911-1920. doi:10.1185/030079906X132488

Freynhagen, R., Tolle, T. R., Gockel, U., & Baron, R. (2016). The painDETECT project - far more than a screening tool on neuropathic pain. *Curr Med Res Opin*, 32(6), 1033-1057. doi:10.1185/03007995.2016.1157460

Frot, M., Faillenot, I., & Mauguiere, F. (2014). Processing of nociceptive input from posterior to anterior insula in humans. *Hum Brain Mapp*, 35(11), 5486-5499. doi:10.1002/hbm.22565

Garcia, D. (2010). Robust smoothing of gridded data in one and higher dimensions with missing values. *Comput Stat Data Anal*, 54(4), 1167-1178. doi:10.1016/j.csda.2009.09.020

Gussew, A., Rzanny, R., Gullmar, D., Scholle, H. C., & Reichenbach, J. R. (2011). 1H-MR spectroscopic detection of metabolic changes in pain processing brain regions in the presence of non-specific chronic low back pain. *Neuroimage*, 54(2), 1315-1323. doi:10.1016/j.neuroimage.2010.09.039

Harfeldt, K., Alexander, L., Lam, J., Mansson, S., Westergren, H., Svensson, P., . . . Alstergren, P. (2018). Spectroscopic differences in posterior insula in patients with chronic temporomandibular pain. *Scand J Pain*, 18(3), 351-361. doi:10.1515/sjpain-2017-0159

Harris, R. E., Napadow, V., Huggins, J. P., Pauer, L., Kim, J., Hampson, J., . . . Clauw, D. J. (2013). Pregabalin rectifies aberrant brain chemistry, connectivity, and functional response in chronic pain patients. *Anesthesiology*, 119(6), 1453-1464. doi:10.1097/aln.0000000000000017

Harris, R. E., Sundgren, P. C., Craig, A. D., Kirshenbaum, E., Sen, A., Napadow, V., & Clauw, D. J. (2009). Elevated insular glutamate in fibromyalgia is associated with experimental pain. *Arthritis Rheum*, 60(10), 3146-3152. doi:10.1002/art.24849

Hubbard, C. S., Lazaridou, A., Cahalan, C. M., Kim, J., Edwards, R. R., Napadow, V., & Loggia, M. L. (2020). Aberrant Salience? Brain Hyperactivation in Response to Pain Onset and Offset in Fibromyalgia. *Arthritis Rheumatol*, 72(7), 1203-1213. doi:10.1002/art.41220

Ip, I. B., Berrington, A., Hess, A. T., Parker, A. J., Emir, U. E., & Bridge, H. (2017). Combined fMRI-MRS acquires simultaneous glutamate and BOLD-fMRI signals in the human brain. *Neuroimage*, 155, 113-119. doi:10.1016/j.neuroimage.2017.04.030

Juchem, C., Cudalbu, C., de Graaf, R. A., Gruetter, R., Henning, A., Hetherington, H. P., & Boer, V. O. (2020). B0 shimming for in vivo magnetic resonance spectroscopy: Experts' consensus recommendations. *NMR Biomed*, e4350. doi:10.1002/nbm.4350

Jung, C., Ichesco, E., Ratai, E. M., Gonzalez, R. G., Burdo, T., Loggia, M. L., . . . Napadow, V. (2020). Magnetic resonance imaging of neuroinflammation in chronic pain: a role for astrogliosis? *Pain*, 161(7), 1555-1564. doi:10.1097/j.pain.0000000000001815

Kameda, T., Fukui, S., Tominaga, R., Sekiguchi, M., Iwashita, N., Ito, K., . . . Konno, S. I. (2018). Brain Metabolite Changes in the Anterior Cingulate Cortex of Chronic Low Back Pain Patients and Correlations Between Metabolites and Psychological State. *Clin J Pain*, 34(7), 657-663. doi:10.1097/AJP.0000000000000583

Katz, P., Pedro, S., & Michaud, K. (2017). Performance of the Patient-Reported Outcomes Measurement Information System 29-Item Profile in Rheumatoid Arthritis, Osteoarthritis, Fibromyalgia, and Systemic Lupus Erythematosus. *Arthritis Care Res (Hoboken)*, 69(9), 1312-1321. doi:10.1002/acr.23183

Kim, H., Kim, J., Loggia, M. L., Cahalan, C., Garcia, R. G., Vangel, M. G., . . . Napadow, V. (2015a). Fibromyalgia is characterized by altered frontal and cerebellar structural covariance brain networks. *Neuroimage Clin*, 7, 667-677. doi:10.1016/j.nicl.2015.02.022

Kim, J., Loggia, M. L., Cahalan, C. M., Harris, R. E., Beissner, F. D. P. N., Garcia, R. G., . . . Napadow, V. (2015b). The somatosensory link in fibromyalgia: functional connectivity of the primary somatosensory cortex is altered by sustained pain and is associated with clinical/autonomic dysfunction. *Arthritis Rheumatol*, 67(5), 1395-1405. doi:10.1002/art.39043

Kim, J., Mawla, I., Kong, J., Lee, J., Gerber, J., Ortiz, A., . . . Napadow, V. (2019). Somatotopically specific primary somatosensory connectivity to salience and default mode networks encodes clinical pain. *Pain*, 160(7), 1594-1605. doi:10.1097/j.pain.0000000000001541

Lee, J., Eun, S., Kim, J., Lee, J. H., & Park, K. (2019). Differential Influence of Acupuncture Somatosensory and Cognitive/Affective Components on Functional Brain Connectivity and Pain Reduction During Low Back Pain State. *Front Neurosci*, 13, 1062. doi:10.3389/fnins.2019.01062

Lee, J., Protsenko, E., Lazaridou, A., Franceschelli, O., Ellingsen, D. M., Mawla, I., . . . Napadow, V. (2018). Encoding of Self-Referential Pain Catastrophizing in the Posterior Cingulate Cortex in Fibromyalgia. *Arthritis Rheumatol*, 70(8), 1308-1318. doi:10.1002/art.40507

Loggia, M. L., Berna, C., Kim, J., Cahalan, C. M., Gollub, R. L., Wasan, A. D., . . . Napadow, V. (2014). Disrupted brain circuitry for pain-related reward/punishment in fibromyalgia. *Arthritis Rheumatol*, 66(1), 203-212. doi:10.1002/art.38191

Loggia, M. L., Kim, J., Gollub, R. L., Vangel, M. G., Kirsch, I., Kong, J., . . . Napadow, V. (2013). Default mode network connectivity encodes clinical pain: an arterial spin labeling study. *Pain*, 154(1), 24-33. doi:10.1016/j.pain.2012.07.029

Lourenco, S., Costa, L., Rodrigues, A. M., Carnide, F., & Lucas, R. (2015). Gender and psychosocial context as determinants of fibromyalgia symptoms (fibromyalgia research criteria) in young adults from the general population. *Rheumatology (Oxford)*, 54(10), 1806-1815. doi:10.1093/rheumatology/kev110

Lu, C., Yang, T., Zhao, H., Zhang, M., Meng, F., Fu, H., . . . Xu, H. (2016). Insular Cortex is Critical for the Perception, Modulation, and Chronification of Pain. *Neurosci Bull*, 32(2), 191-201. doi:10.1007/s12264-016-0016-y

Lv, K., Song, W., Tang, R., Pan, Z., Zhang, Y., Xu, Y., . . . Xu, M. (2018). Neurotransmitter alterations in the anterior cingulate cortex in Crohn's disease patients with abdominal pain: A preliminary MR spectroscopy study. *Neuroimage Clin*, 20, 793-799. doi:10.1016/j.nicl.2018.09.008

Madhavarao, C. N., Chinopoulos, C., Chandrasekaran, K., & Namboodiri, M. A. (2003). Characterization of the N-acetylaspartate biosynthetic enzyme from rat brain. *J Neurochem*, 86(4), 824-835. doi:10.1046/j.1471-4159.2003.01905.x

Maudsley, A. A., Andronesi, O. C., Barker, P. B., Bizzi, A., Bogner, W., Henning, A., . . . Soher, B. J. (2020). Advanced magnetic resonance spectroscopic neuroimaging: Experts' consensus recommendations. *NMR Biomed*, e4309. doi:10.1002/nbm.4309

Meints, S. M., Mawla, I., Napadow, V., Kong, J., Gerber, J., Chan, S. T., . . . Edwards, R. R. (2019). The relationship between catastrophizing and altered pain sensitivity in patients with chronic low-back pain. *Pain*, 160(4), 833-843. doi:10.1097/j.pain.0000000000001461

Mok, L. C., & Lee, I. F. (2008). Anxiety, depression and pain intensity in patients with low back pain who are admitted to acute care hospitals. *J Clin Nurs*, 17(11), 1471-1480. doi:10.1111/j.1365-2702.2007.02037.x

Morel, A., Gallay, M. N., Baechler, A., Wyss, M., & Gallay, D. S. (2013). The human insula: Architectonic organization and postmortem MRI registration. *Neuroscience*, 236, 117-135. doi:10.1016/j.neuroscience.2012.12.076

Napadow, V., & Harris, R. E. (2014). What has functional connectivity and chemical neuroimaging in fibromyalgia taught us about the mechanisms and management of 'centralized' pain? *Arthritis Res Ther*, 16(5), 425. doi:10.1186/s13075-014-0425-0

Napadow, V., LaCount, L., Park, K., As-Sanie, S., Clauw, D. J., & Harris, R. E. (2010). Intrinsic brain connectivity in fibromyalgia is associated with chronic pain intensity. *Arthritis Rheum*, 62(8), 2545-2555. doi:10.1002/art.27497

Nordengen, K., Heuser, C., Rinholm, J. E., Matalon, R., & Gundersen, V. (2015). Localisation of N-acetylaspartate in oligodendrocytes/myelin. *Brain Struct Funct*, 220(2), 899-917. doi:10.1007/s00429-013-0691-7

Oz, G., Deelchand, D. K., Wijnen, J. P., Mlynarik, V., Xin, L., Mekle, R., . . . Experts' Working Group on Advanced Single Voxel, H. M. (2020). Advanced single voxel (1) H magnetic resonance spectroscopy techniques in humans: Experts' consensus recommendations. *NMR Biomed*, e4236. doi:10.1002/nbm.4236

Peek, A. L., Rebbeck, T., Puts, N. A., Watson, J., Aguila, M. R., & Leaver, A. M. (2020). Brain GABA and glutamate levels across pain conditions: A systematic literature review and meta-analysis of 1H-MRS studies using the MRS-Q quality assessment tool. *Neuroimage*, 210, 116532. doi:10.1016/j.neuroimage.2020.116532

Petrou, M., Harris, R. E., Foerster, B. R., McLean, S. A., Sen, A., Clauw, D. J., & Sundgren, P. C. (2008). Proton MR spectroscopy in the evaluation of cerebral metabolism in patients with fibromyalgia: comparison with healthy controls and correlation with symptom severity. *AJNR Am J Neuroradiol*, 29(5), 913-918. doi:10.3174/ajnr.A0959

Provencher, S. W. (1993). Estimation of metabolite concentrations from localized in vivo proton NMR spectra. *Magn Reson Med*, 30(6), 672-679. doi:10.1002/mrm.1910300604

Rae, C. D. (2014). A guide to the metabolic pathways and function of metabolites observed in human brain 1H magnetic resonance spectra. *Neurochem Res*, 39(1), 1-36. doi:10.1007/s11064-013-1199-5

Ratai, E. M., Alshikho, M. J., Zurcher, N. R., Loggia, M. L., Cebulla, C. L., Cernasov, P., . . . Atassi, N. (2018). Integrated imaging of [(11)C]-PBR28 PET, MR diffusion and magnetic resonance spectroscopy (1)H-MRS in amyotrophic lateral sclerosis. *Neuroimage Clin*, 20, 357-364. doi:10.1016/j.nicl.2018.08.007

Setiawan, E., Wilson, A. A., Mizrahi, R., Rusjan, P. M., Miler, L., Rajkowska, G., . . . Meyer, J. H. (2015). Role of translocator protein density, a marker of neuroinflammation, in the brain during major depressive episodes. *JAMA Psychiatry*, 72(3), 268-275. doi:10.1001/jamapsychiatry.2014.2427

Simis, M., Reidler, J. S., Duarte Macea, D., Moreno Duarte, I., Wang, X., Lenkinski, R., . . . Fregni, F. (2015). Investigation of central nervous system dysfunction in chronic pelvic

pain using magnetic resonance spectroscopy and noninvasive brain stimulation. *Pain Pract*, 15(5), 423-432. doi:10.1111/papr.12202

Sorensen, L., Siddall, P. J., Trenell, M. I., & Yue, D. K. (2008). Differences in metabolites in pain-processing brain regions in patients with diabetes and painful neuropathy. *Diabetes Care*, 31(5), 980-981. doi:10.2337/dc07-2088

Staud, R., Robinson, M. E., & Price, D. D. (2007). Temporal summation of second pain and its maintenance are useful for characterizing widespread central sensitization of fibromyalgia patients. *J Pain*, 8(11), 893-901. doi:10.1016/j.jpain.2007.06.006

Sullivan, M. J., Bishop, S. R., & Pivik, J. (1995). The pain catastrophizing scale: development and validation. *Psychological assessment*, 7(4), 524.

Torrado-Carvajal, A., Albrecht, D. S., Lee, J., Andronesi, O. C., Ratai, E. M., Napadow, V., & Loggia, M. L. (2020). Inpainting as a Technique for Estimation of Missing Voxels in Brain Imaging. *Ann Biomed Eng*. doi:10.1007/s10439-020-02556-3

Valdes, M., Collado, A., Bargallo, N., Vazquez, M., Rami, L., Gomez, E., & Salamero, M. (2010). Increased glutamate/glutamine compounds in the brains of patients with fibromyalgia: a magnetic resonance spectroscopy study. *Arthritis Rheum*, 62(6), 1829-1836. doi:10.1002/art.27430

Wang, Y., Li, D., Bao, F., Ma, S., Guo, C., Jin, C., & Zhang, M. (2014). Thalamic metabolic alterations with cognitive dysfunction in idiopathic trigeminal neuralgia: a multivoxel spectroscopy study. *Neuroradiology*, 56(8), 685-693. doi:10.1007/s00234-014-1376-5

Wilson, M., Andronesi, O., Barker, P. B., Bartha, R., Bizzi, A., Bolan, P. J., . . . Howe, F. A. (2019). Methodological consensus on clinical proton MRS of the brain: Review and recommendations. *Magn Reson Med*, 82(2), 527-550. doi:10.1002/mrm.27742

Wolfe, F., Clauw, D. J., Fitzcharles, M. A., Goldenberg, D. L., Katz, R. S., Mease, P., . . . Yunus, M. B. (2010). The American College of Rheumatology preliminary diagnostic criteria for fibromyalgia and measurement of symptom severity. *Arthritis Care Res (Hoboken)*, 62(5), 600-610. doi:10.1002/acr.20140

Figure Legends

Figure 1. Magnetic Resonance Spectral Imaging (MRSI) data collection. (A) Volume of interest (VOI) was placed manually to cover the bilateral insular and cingulate cortices, and thalami. The overlay shows spatial distribution for overlapped collected voxels across participants (FM and HC), and data analysis was performed only for voxels with contribution from 100% of participants. (B) Sample spectra (thin black line, fit in the range of 4.2 to 1.8 ppm) from a right mid-insular cortex voxel is presented (SNR = 15 and FWHM = 0.040 ppm for this example), with LCModel fit (thick red line). The average values and percentage of 'low'- and 'adquate'-quality data voxels for SNR and FWHM were reported for quality measurement in the same region (SNR: 'low'-quality data voxels = 4.56 ± 1.29, 29.17%, 'adequate'-quality data voxels = 7.28 ± 1.85, 70.83%; FWHM: 'low'-quality data voxels = 0.11 ± 0.02 ppm, 23.33%, 'adequate'-quality data voxels = 0.07 ± 0.01 ppm, 76.67%). L = left hemisphere, NAA = N-acetylaspartate, NAAG = N-acetylaspartylglutamate, Glu = glutamate, Gln = glutamine, mIno = myo-inositol, Cr = creatine, PCr = phosphocreatine, GPC = glycerophosphocholine, pCho = phosphocholine).

Figure 2. Study flowchart. Glx = combined glutamate and glutamine concentration, mIno = myo-inositol concentration, tNAA = combined N-acetylaspartate and N-acetylaspartylglutamate concentration, tCr = combined creatine and phosphocreatine concentration.

Figure 3. Spatial distribution of 'low'-quality data voxels (SNR < 5, FWHM ≥ 0.1 ppm, *or* CRLB ≥ 20%) for Glx/tCr with N = 86 (A), mIno/tCr with N = 85 (B), and tNAA/tCr with N = 87 (C) in FM. The majority of 'low'-quality data voxels were found in the ventromedial part of the VOI and ventricles. L = left hemisphere, Glx = combined glutamate and glutamine concentration, mIno = myo-inositol concentration, tNAA = combined N-acetylaspartate and N-acetylaspartylglutamate concentration, tCr = combined creatine and phosphocreatine concentration.

Figure 4. Brain Glx/tCr correlates of PCS scores (A) and BPI severity scores (B). Significant positive correlations between PCS scores and Glx/tCr levels in the anterior and middle insular cortices (A), and BPI severity and Glx/tCr levels in the middle/posterior insular and posterior cingulate cortices (B) were found. N.b. Correlation plots were shown for black border voxel. L =

left hemisphere, PCS = pain catastrophizing scale, BPI = Brief Pain Inventory, Glx = combined glutamate and glutamine concentration, tCr = combined creatine and phosphocreatine concentration. Age, gabapentin/pregabalin usage, and average tCr level were controlled.

Figure 5. Brain mIno/tCr correlates of PCS scores (A) and BPI severity scores (B). Significant negative correlations between PCS scores and mIno/tCr levels in the posterior cingulate cortex (A), and BPI severity scores and mIno/tCr levels in the anterior midcingulate cortex and thalamus (B) were found. N.b. Correlation plots were shown for black border voxels. Significant voxels from the cluster-correction for multiple comparisons ($Z > 2.3$, $P < 0.05$) were highlighted with a red border. L = left hemisphere, PCS = pain catastrophizing scale, BPI = brief pain inventory, mIno = myo-inositol concentration, tCr = combined creatine and phosphocreatine concentration. Age, gabapentin/pregabalin usage, and average tCr level were controlled.

Figure 6. Brain tNAA/tCr correlates of clinical pain measures. Metabolite concentrations of tNAA/tCr were positively correlated with (A) PCS scores in the middle and anterior insular cortices and negatively correlated with (B) BPI severity scores in the anterior midcingulate cortex. (C) Positive correlations between tNAA/tCr levels and Cuff P40 pressure were found in the posterior insular cortex, anterior/posterior middle and posterior cingulate cortices, and thalamus. N.b. Correlation plots were shown for black border voxels. Significant voxels from the cluster-correction for multiple comparisons ($Z > 2.3$, $P < 0.05$) were highlighted with a red border. L = left hemisphere, R = right hemisphere, PCS = pain catastrophizing scale, BPI = brief pain inventory, tNAA = combined N-acetylaspartate and N-acetylaspartylglutamate concentration, tCr = combined creatine and phosphocreatine concentration. Age, gabapentin/pregabalin usage, and average tCr level were controlled.

Table1. Demographics and clinical/behavioral variables

	FM (N = 87) Mean ± SD (min-max)	HC (N = 33) Mean ± SD (min-max)	FM vs. HC P-value[a]
Demographics			
Age (years)	40.7 ± 12.2 (18-65)	37.6 ± 12.7 (22-63)	0.23
Clinical pain measures			
Pain Catastrophizing Scale (total, from 0 to 52)	24.1 ± 11.6 (0-48)	8.1 ± 8.0 (0-29)	0.003
Brief Pain Inventory (Severity, from 0 to 10)[b]	5.1 ± 1.7 (1.75-10)	N/A	N/A
Cuff P40 pressure (mmHg, 40 /100)[c]	147.0 ± 52.8 (30-300)	184.6 ± 72.1 (65-400)	0.003
FM-specific variables			
FM duration (years)[d]	6.6 ± 6.0 (0.1-25.6)	N/A	N/A
Pain intensity at study visit (from 0 to 100)	45.2 ± 18.2 (0-80)	N/A	N/A
FIQR (total, from 0 to 100)[e]	56.9 ± 16.8 (17.6-90.3)	N/A	N/A
painDETECT (total score, from -1 to 38)	17.8 ± 7.1 (2-34)	N/A	N/A
PROMIS-29 (physical function, from 22.5 to 57, t-score)[f]	35.3 ± 4.8 (22.9-45.3)	N/A	N/A

[a]Significance ($P < 0.05$) was determined using a Student's *t*-test. [b]BPI was collected from 86 FM patients, and this measure is not applicable (N/A) in HC. [c]Cuff pressure was individually tailored at left lower leg (targeted at 40/100, 0 = no pain, 100 = worst pain imaginable) and was collected from 75 FM patients and 33 HC. [d]FM duration, [e]FIQR, and [f]PROMIS-29 were collected from 84, 86, and 83 FM patients, respectively. FIQR = Revised Fibromyalgia Impact Questionnaire, PROMIS-29 = Patient-Reported Outcomes Measurement Information System.

Table2. Brain metabolite correlates of clinical/behavioral variables in FM

	Side	MNI coordinates, mm X	Y	Z	Z score[a]	%inpaint[b]	P(r)[c]
Glx/tCr vs. PCS (N=86)							
insula, anterior	L	-42	5.25	7.5	3.04	48.0	0.029
insula, middle	R	40.5	-2.25	0	2.66	52.0	0.009
Glx/tCr vs. BPI severity (N=85)							
insula, middle	R	40.5	-9.75	15	2.49	20.0	0.037
cingulate, posterior	L	-4.5	-47.25	30	2.42	19.0	0.007
mIno/tCr vs. PCS (N=85)							
cingulate, posterior	R	3	-39.75	37.5	-2.58	14.0	0.035
mIno/tCr vs. BPI severity (N=84)							
midcingulate, anterior	***L***	***-12***	***27.75***	***22.5***	***-3.60***	***54.0***	***0.016***
thalamus	***R***	***10.5***	***-2.25***	***7.5***	***-2.54***	***52.0***	***0.015***
tNAA/tCr vs. PCS (N=87)							
insula, anterior	L	-42	5.25	7.5	2.98	16.1	0.010
insula, middle	R	40.5	-2.25	0	3.19	44.8	0.004
insula, middle	L	-42	-2.25	0	2.51	57.5	0.049
tNAA/tCr vs. BPI severity (N=86)							
midcingulate, anterior	L	-12	27.75	22.5	-3.11	20.9	0.034
tNAA/tCr vs. Cuff P40 pressure (N=75)							

insula, posterior	***R***	***33***	***-24.75***	***15***	***2.63***	***0.0***	***0.010***
midcingulate	L	-4.5	5.25	30	2.52	10.7	0.004
cingulate, posterior	***L***	***-4.5***	***-47.25***	***22.5***	***3.07***	***4.0***	***0.004***
thalamus	L	-4.5	-17.25	15	2.54	25.3	0.024

N.b. Results were controlled for age, gabapentin/pregabalin usage, and average tCr level. Significant local maxima were reported. Results from cluster-correction for multiple comparisons ($Z > 2.3$, $P < 0.05$) were highlighted (***bold italicized***). [a]Z scores were reported (absolute value > 2.3). [b]Percentage of inpainted data points (*i.e.*, patients) in the entire dataset (< 60%). [c]Significance of correlation analysis between metabolite concentration levels and clinical pain measures (using non-inpainted data points only, $P \leq 0.05$). L = left hemisphere, R = right hemisphere, Glx = combined glutamate and glutamine concentration, mIno = myo-inositol concentration, tNAA = combined N-acetylaspartate and N-acetylaspartylglutamate concentration, tCr = combined creatine and phosphocreatine concentration, PCS = pain catastrophizing scale, BPI = Brief Pain Inventory.

(a)

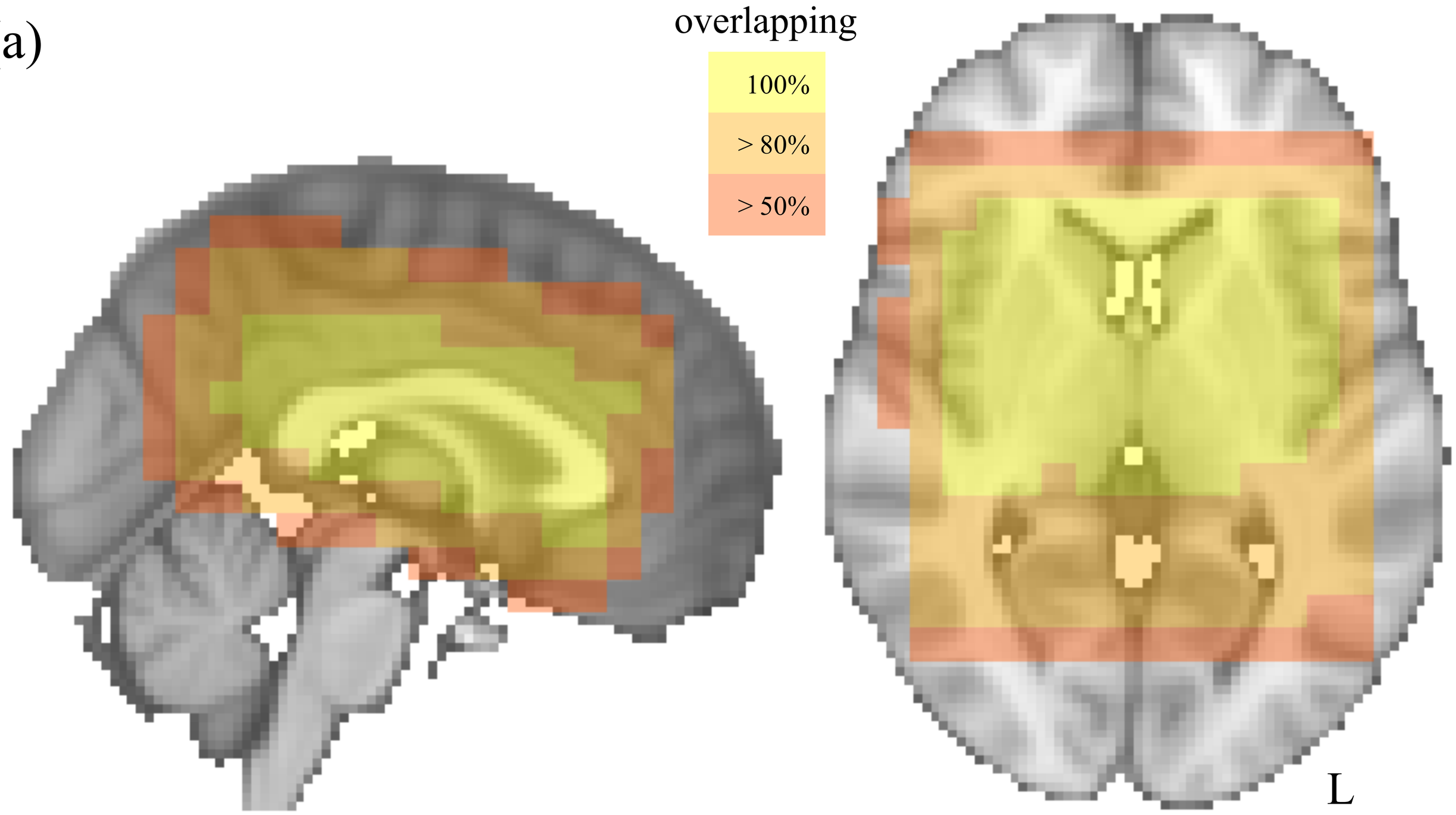
overlapping
100%
> 80%
> 50%
L

X = 0 mm

Z = 5 mm

(b)

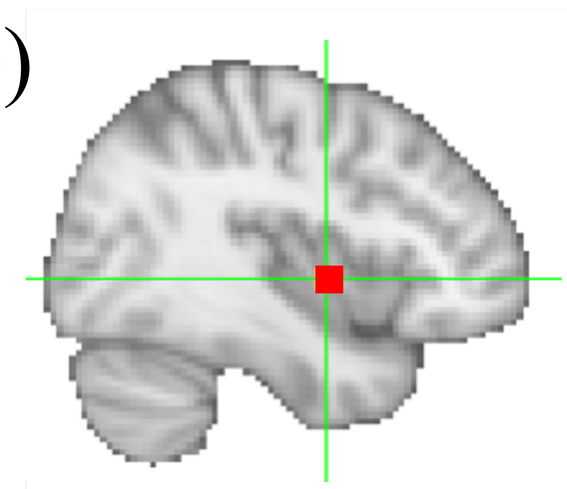

NAA
+NAAG
Cr+PCr
GPC+PCho
Cr+PCr
mIno
Glu+Gln
4.2
4.0
3.8
3.6
3.4
3.2
3.0
2.8
2.6
2.4
2.2
2.0
1.8
Chemical Shift (ppm)

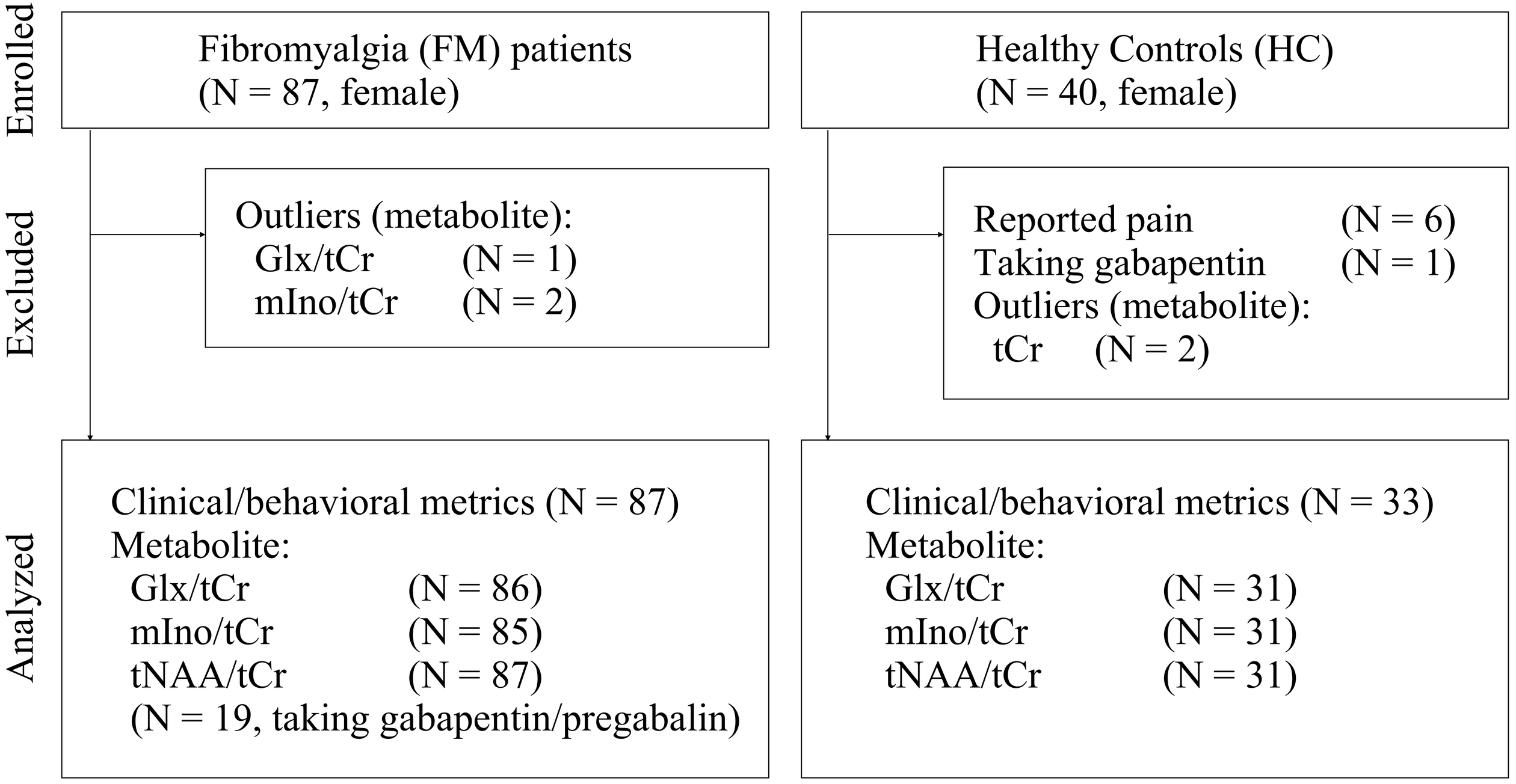
Enrolled
Fibromyalgia (FM) patients
(N = 87, female)
Healthy Controls (HC)
(N = 40, female)
Excluded
Outliers (metabolite):
Glx/tCr (N = 1)
mIno/tCr (N = 2)
Reported pain (N = 6)
Taking gabapentin (N = 1)
Outliers (metabolite):
tCr (N = 2)
Analyzed
Clinical/behavioral metrics (N = 87)
Metabolite:
Glx/tCr (N = 86)
mIno/tCr (N = 85)
tNAA/tCr (N = 87)
(N = 19, taking gabapentin/pregabalin)
Clinical/behavioral metrics (N = 33)
Metabolite:
Glx/tCr (N = 31)
mIno/tCr (N = 31)
tNAA/tCr (N = 31)

(a)

‘Low’-quality data voxels

100%

> 80%

≥ 60%

< 60%

(b)

(c)

L

X = 0 mm

Z = 5 mm

(a)

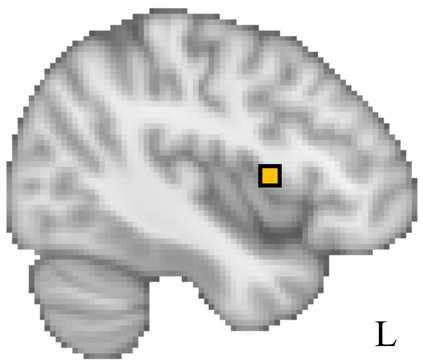

X = -42 mm

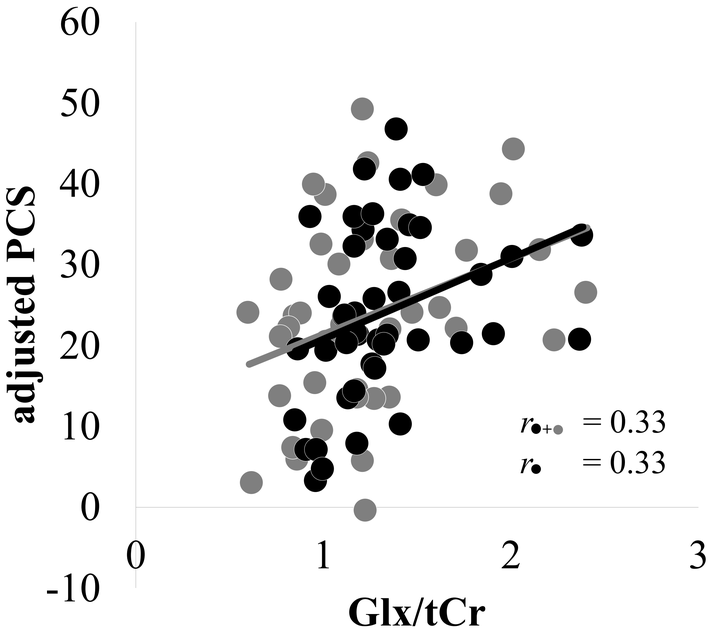

Z stat

2.3 4

-2.3 -4

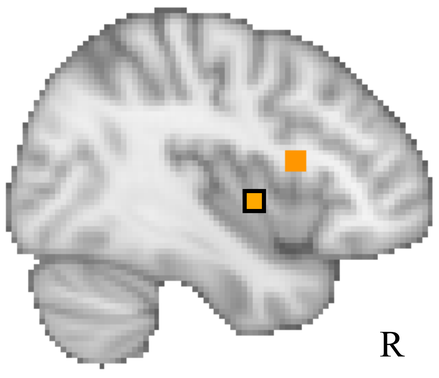

X = 40.5 mm

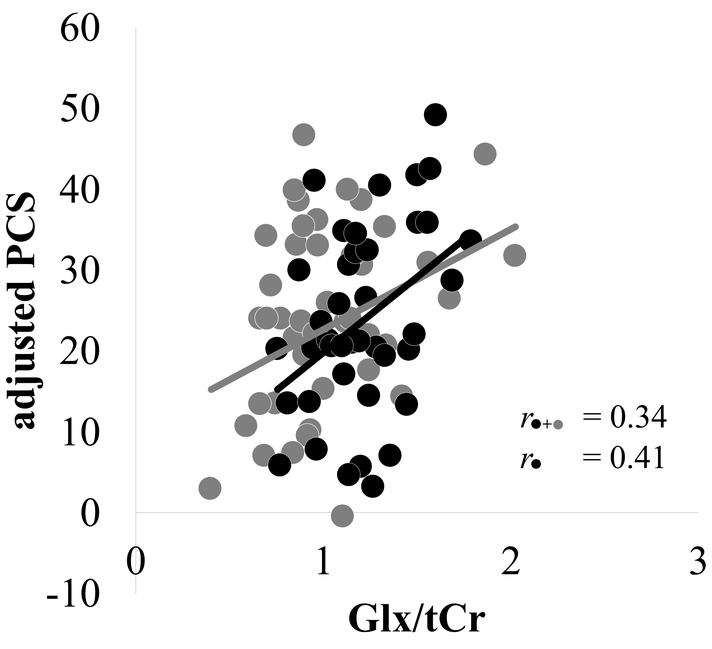

(b)

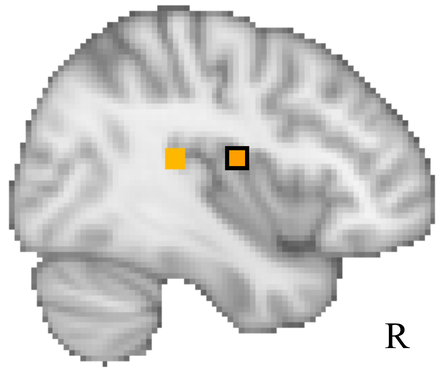

X = 40.5 mm

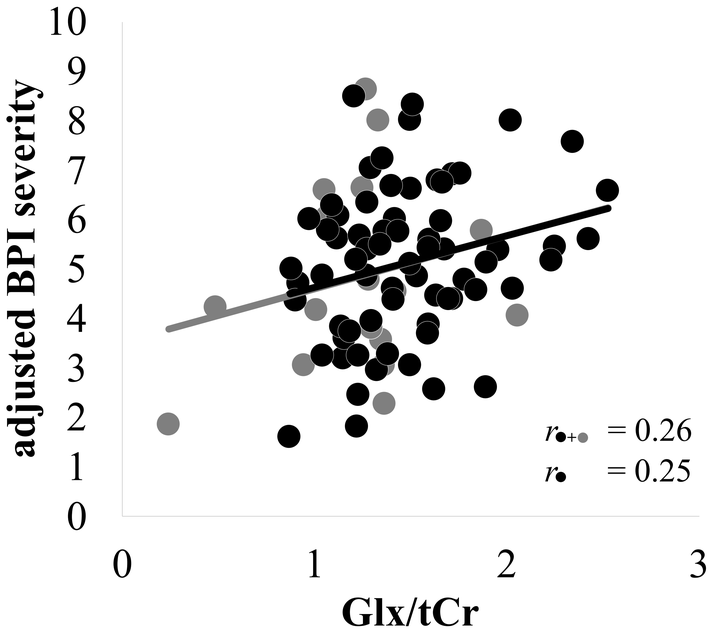

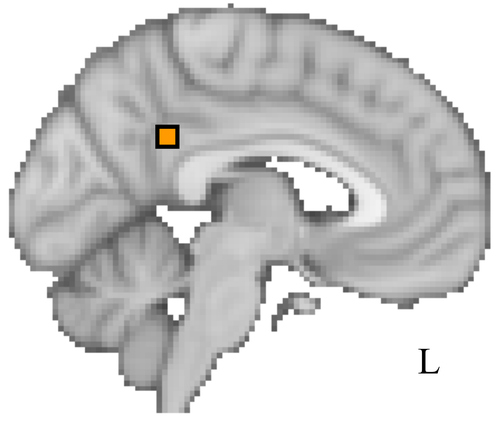

X = -4.5 mm

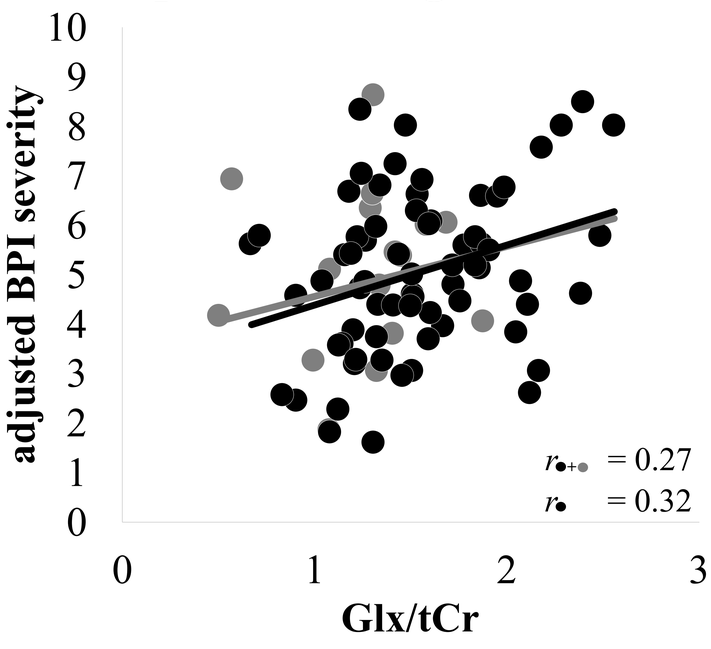

non-inpainted data ('adequate' quality)

inpainted data ('low' quality)

inpainted + non-inpainted linear fit

non-inpainted only linear fit

(a)

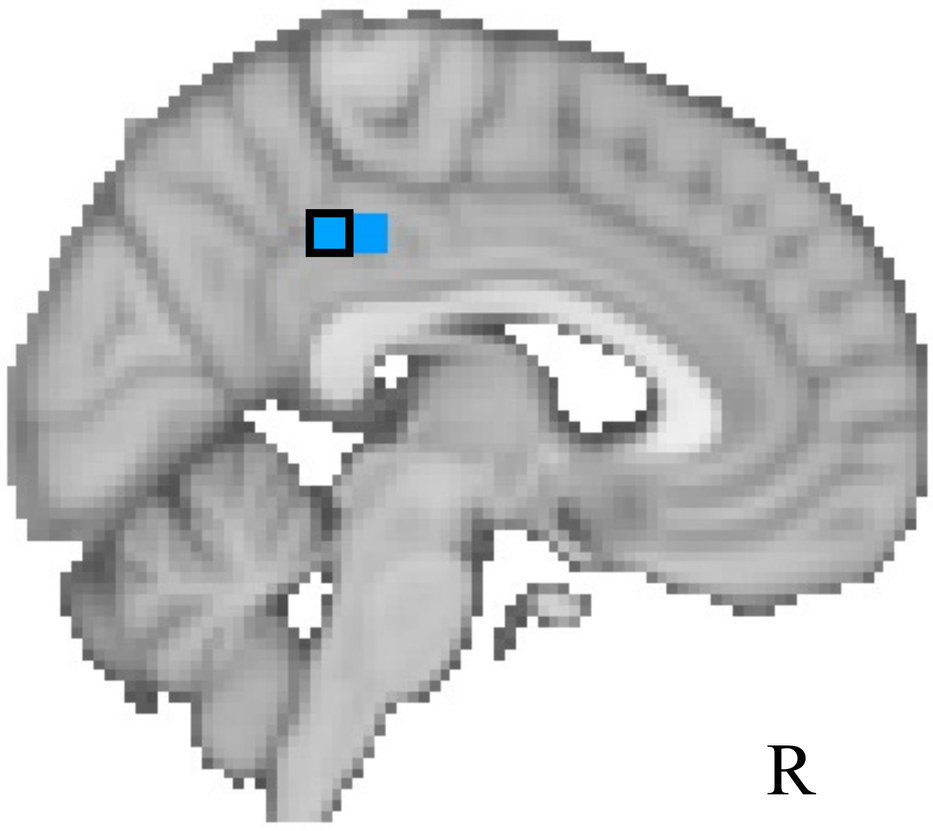

Z = 3 mm

R

(b)

Z stat
2.3 4
-2.3 -4

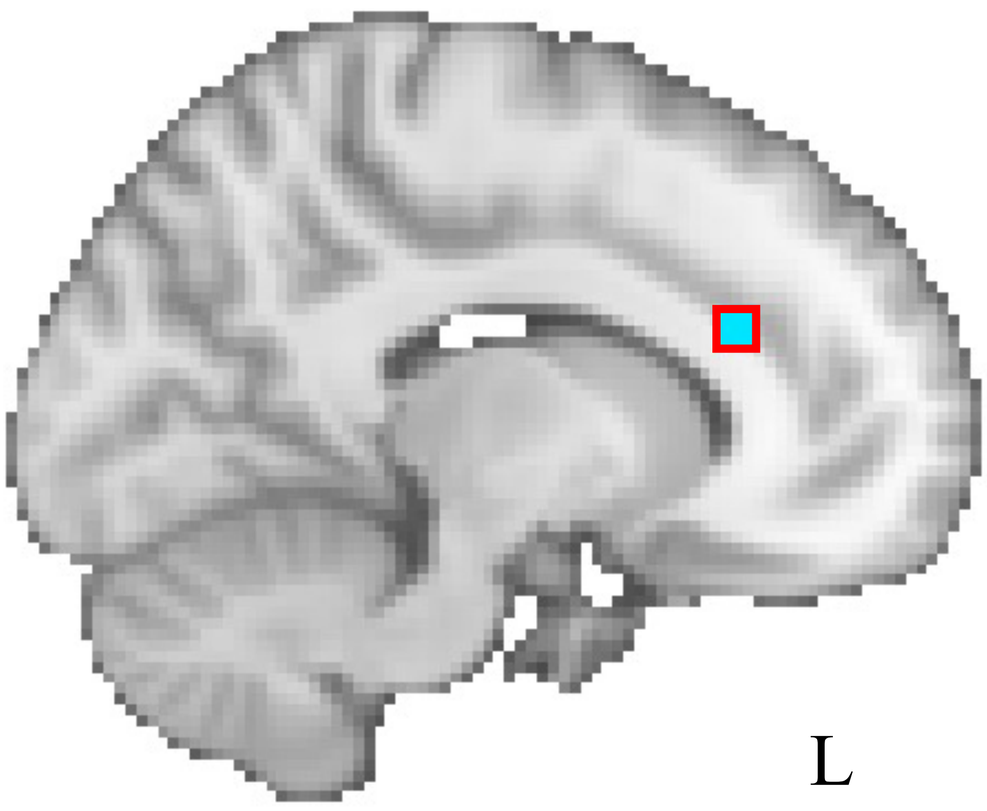

X = -12 mm

L

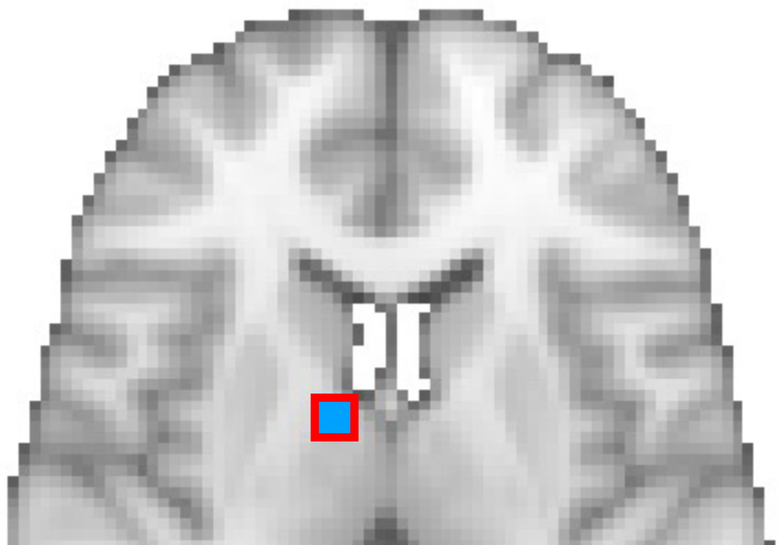

Z = 7.5 mm

R

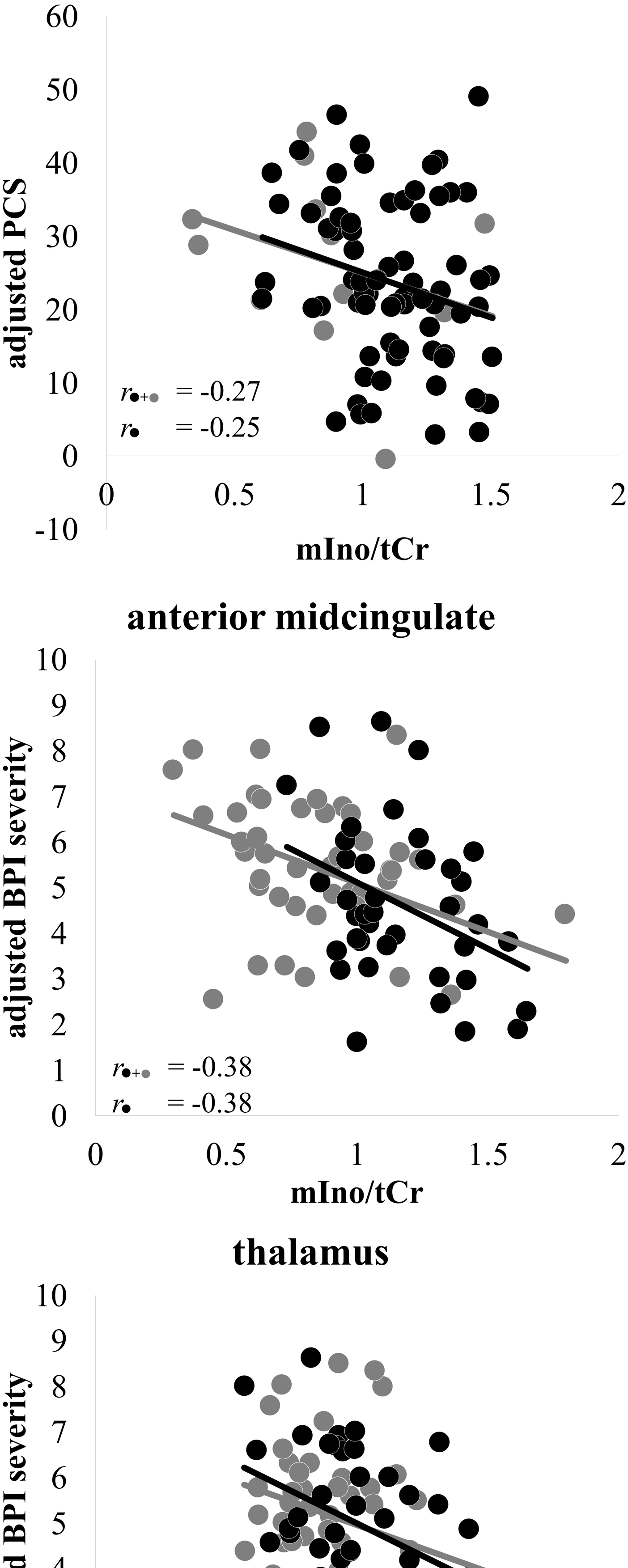

(a)

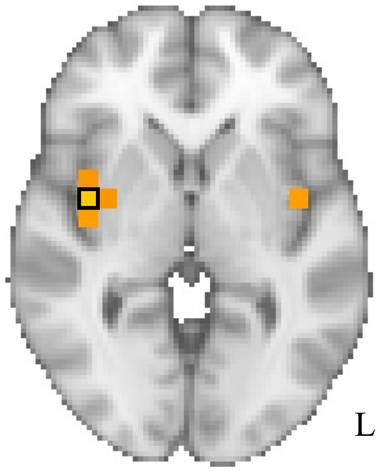

Z = 0 mm

middle insular

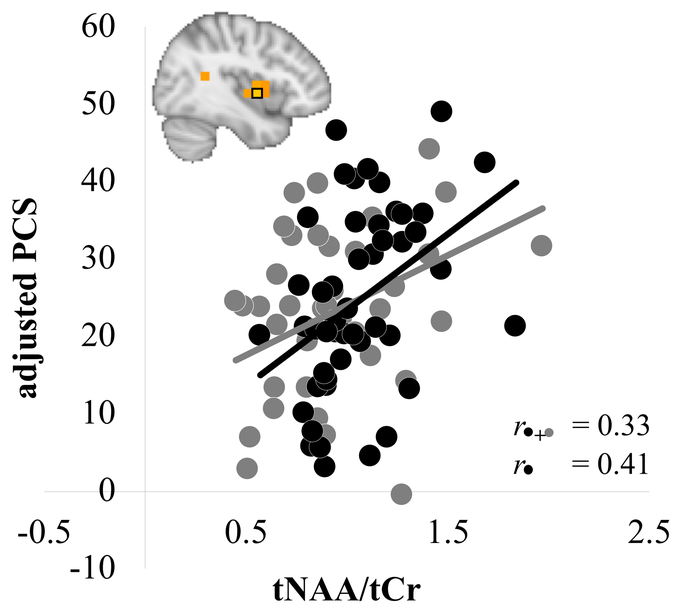

Z stat
2.3 4
-2.3 -4

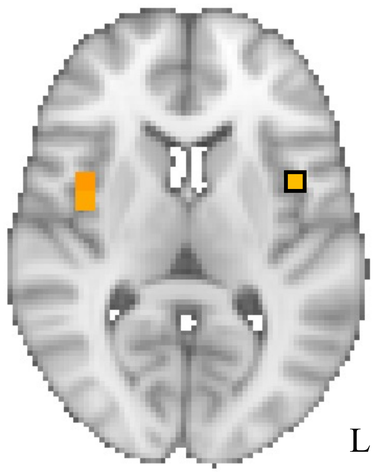

Z = 7.5 mm

anterior insular

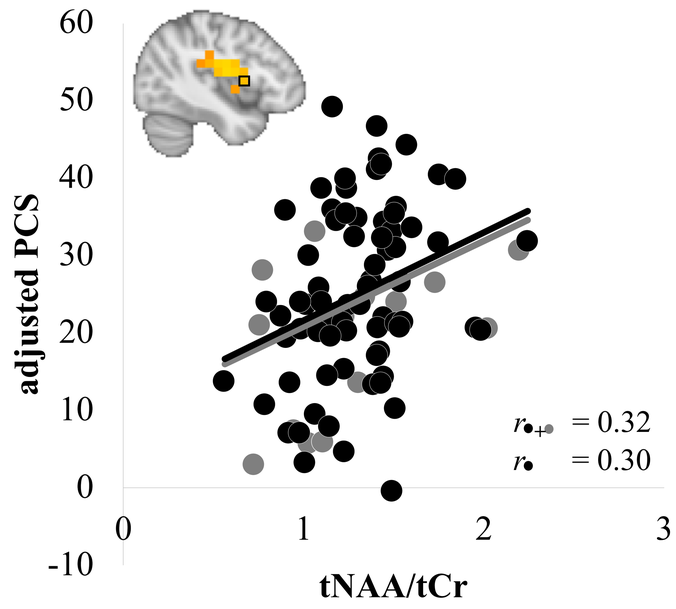

(b)

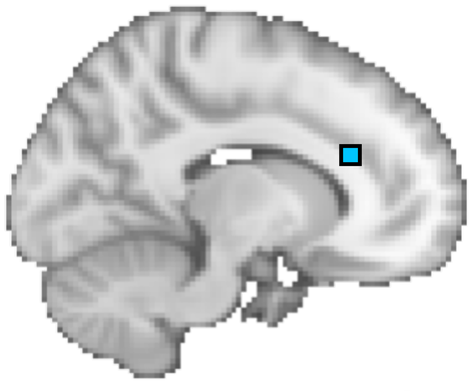

X = -12 mm

anterior midcingulate

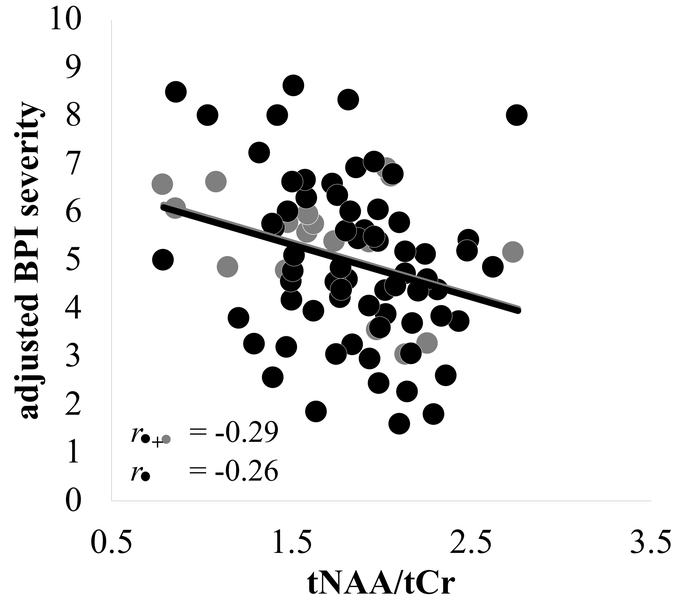

(c)

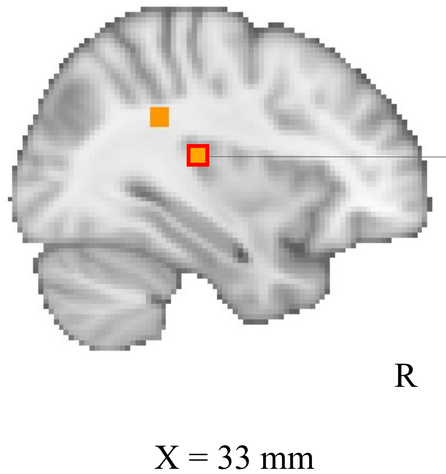

X = 33 mm

posterior insular

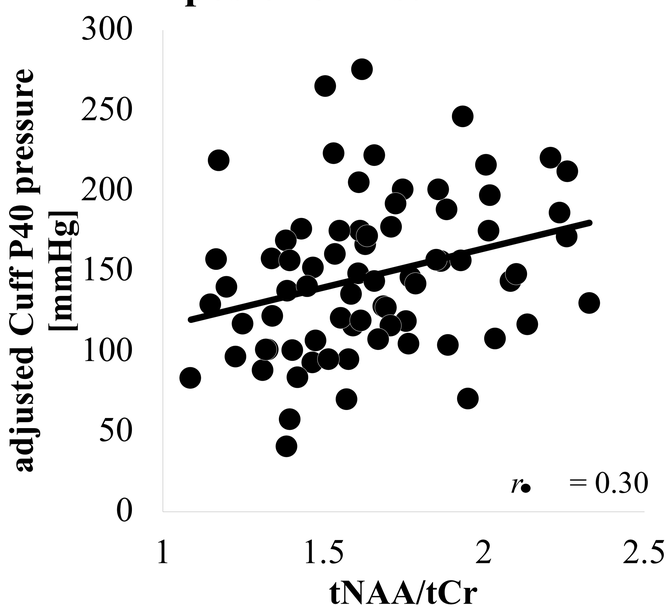

posterior cingulate

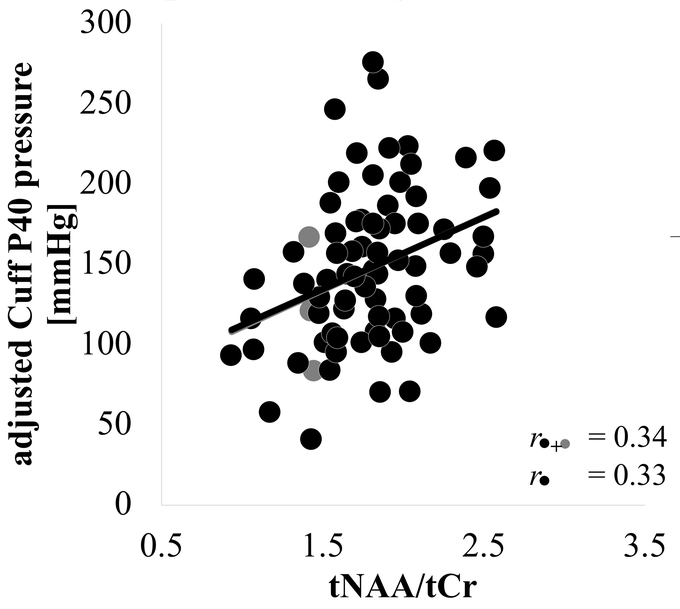

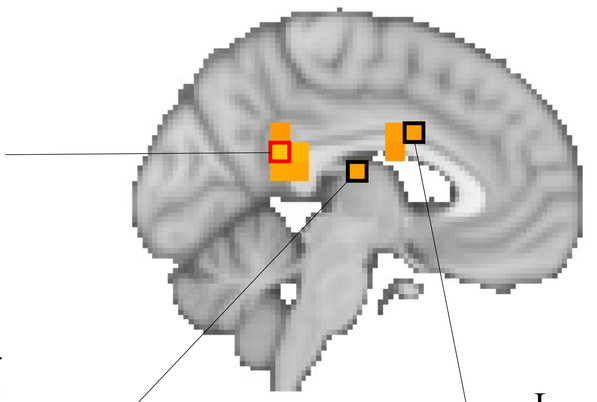

X = -4.5 mm

thalamus

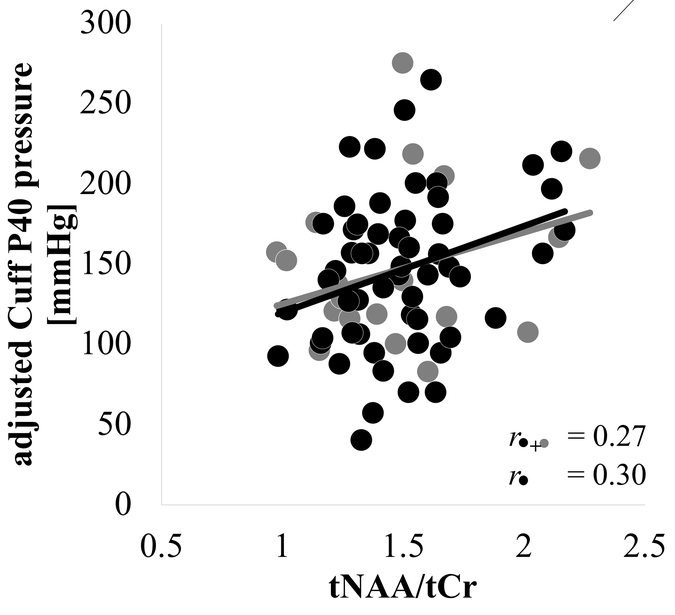

midcingulate

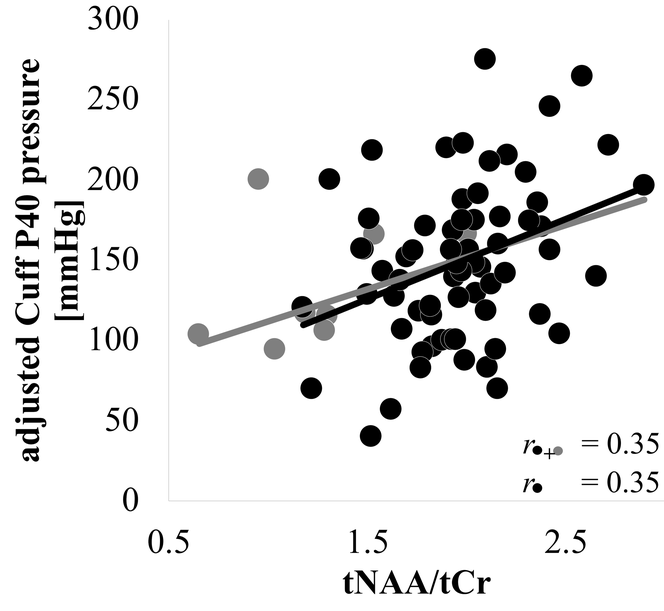

non-inpainted data ('adequate' quality)
inpainted data ('low' quality)
inpainted + non-inpainted linear fit
non-inpainted only linear fit